Signals from the ventrolateral thalamus to the motor cortex during locomotion

Vladimir Marlinski, Wijitha U. Nilaweera, Pavel V. Zelenin, Mikhail G. Sirota and Irina N. Beloozerova

J Neurophysiol 107:455-472, 2012. First published 12 October 2011; doi:10.1152/jn.01113.2010

Journal of Neurophysiology publishes original articles on the function of the nervous system. It is published 12 times a year (monthly) by the American Physiological Society, 9650 Rockville Pike, Bethesda MD 20814-3991. ISSN: 0022-3077, ESSN: 1522-1598. Visit our website at http://www.the-aps.org/.

J Neurophysiol 107: 455–472, 2012.
First published October 12, 2011; doi:10.1152/jn.01113.2010.

Signals from the ventrolateral thalamus to the motor cortex during locomotion

Vladimir Marlinski,[1] Wijitha U. Nilaweera,[1,2] Pavel V. Zelenin,[3] Mikhail G. Sirota,[1] and Irina N. Beloozerova[1]

[1]*Barrow Neurological Institute, St. Joseph's Hospital and Medical Center and* [2]*Arizona State University-Barrow Neurological Institute Interdisciplinary Graduate Program in Neuroscience, Phoenix, Arizona; and* [3]*Department of Neuroscience, Karolinska Institute, Stockholm, Sweden*

Submitted 22 December 2010; accepted in final form 11 October 2011

Marlinski V, Nilaweera WU, Zelenin PV, Sirota MG, Beloozerova IN. Signals from the ventrolateral thalamus to the motor cortex during locomotion. *J Neurophysiol* 107: 455–472, 2012. First published October 12, 2011; doi:10.1152/jn.01113.2010.—The activity of the motor cortex during locomotion is profoundly modulated in the rhythm of strides. The source of modulation is not known. In this study we examined the activity of one of the major sources of afferent input to the motor cortex, the ventrolateral thalamus (VL). Experiments were conducted in chronically implanted cats with an extracellular single-neuron recording technique. VL neurons projecting to the motor cortex were identified by antidromic responses. During locomotion, the activity of 92% of neurons was modulated in the rhythm of strides; 67% of cells discharged one activity burst per stride, a pattern typical for the motor cortex. The characteristics of these discharges in most VL neurons appeared to be well suited to contribute to the locomotion-related activity of the motor cortex. In addition to simple locomotion, we examined VL activity during walking on a horizontal ladder, a task that requires vision for correct foot placement. Upon transition from simple to ladder locomotion, the activity of most VL neurons exhibited the same changes that have been reported for the motor cortex, i.e., an increase in the strength of stride-related modulation and shortening of the discharge duration. Five modes of integration of simple and ladder locomotion-related information were recognized in the VL. We suggest that, in addition to contributing to the locomotion-related activity in the motor cortex during simple locomotion, the VL integrates and transmits signals needed for correct foot placement on a complex terrain to the motor cortex.

cat; activity; walking

THIS STUDY ON THE ACTIVITY of the ventrolateral thalamus (VL) in the walking cat was prompted by the fact that during locomotion the activity of the target of VL projection—the motor cortex—changes periodically in the rhythm of locomotor movements (Armstrong and Drew 1984; Beloozerova and Sirota 1985, 1993a, 1993b; Drew 1993). The origin of this modulation is unclear. In decerebrated cats, it was shown that integrity of the cerebellum is required for all subcortical descending tracts: vestibulo-, reticulo-, and rubro-spinal, to exhibit locomotion-related modulation of their activity (Orlovski 1970; Orlovsky 1972a, 1972b). Neurons of those tracts receive direct synaptic projections from the cerebellum. The motor cortex also gives rise to a major descending tract—the pyramidal tract. The motor cortex does not receive direct input from the cerebellum but receives input from the VL, one synapse away from it. We hypothesized that during locomotion the VL passes locomotion-related information from the cerebellum to the motor cortex. The first goal of this study was to elucidate whether the pattern of activity of VL neurons during locomotion in an uncomplicated environment (simple locomotion) is suitable to contribute to the locomotion-related activity in the motor cortex. We found that the majority of VL neurons were well fit for such a role.

It is known that VL neurons change their activity prior to voluntary movements (Evarts 1971; Kurata 2005; Neafsea et al. 1978; Schmied et al. 1979; Strick 1976; van Donkelaar et al. 1999). We hypothesized that the VL is also involved in voluntary modifications of locomotion. The second goal of this study was to explore whether VL neurons contribute to an increase in modulation of the motor cortex activity that is observed during locomotion over a complex terrain (complex locomotion). On complex terrain, vision is required to adjust steps to irregularities of the walking path. During stepping under visual control the activity of the motor cortex is dramatically different from that during walking on a flat surface, and these changes are crucial for correct stepping on a complex terrain (Beloozerova and Sirota 1988, 1993a; Beloozerova et al. 2010; Drew 1988, 1993). The inputs responsible for the changes of the activity in the motor cortex during complex locomotion compared with simple walking are not clear. We have previously explored whether area 5 of parietal cortex, which is known to integrate visual and motor information for control of limb movements (see, e.g., Buneo and Andersen 2006; Mountcastle 1995), could be responsible for modulation of the motor cortex activity during complex locomotion (Beloozerova and Sirota 2003). We found, however, that the pattern of activity of area 5 neurons was quite different from that of the motor cortex and thus seemed unlikely to be the primary source of modulation. Here we consider another possibility, that during complex locomotion the input from the VL changes. We hypothesized that, in addition to basic locomotion-related information, the VL transmits information that is needed to control landing positions of feet during walking on a complex terrain to the motor cortex. We have found strong evidence supporting this hypothesis.

A brief account of a part of this study was published in abstract form (Beloozerova and Sirota 2002).

METHODS

Extracellular recordings from single VL neurons were obtained during chronic experiments in cats. One adult female (*cat A*) and two adult males (*cats B* and *C*) were used. Methods of surgical preparation and recording technique have been previously described in detail and will be briefly reported here (Beloozerova and Sirota 1993a; Prilutsky et al. 2005; Sirota et al. 2005; Zelenin et al. 2010). The experimental

Address for reprint requests and other correspondence: I. N. Beloozerova, Barrow Neurological Inst., St. Joseph's Hospital and Medical Center, 350 West Thomas Rd., Phoenix, AZ 85013 (e-mail: ibelooz@chw.edu).

protocol was in compliance with National Institutes of Health guidelines for the care and use of animals in research and was approved by the Barrow Neurological Institute Animal Care and Use Committee.

Locomotion Tasks

Two locomotion tasks were used: *1*) simple locomotion on a flat surface and *2*) complex locomotion on crosspieces of a horizontal ladder. It has been demonstrated in several studies that simple locomotion does not require vision, while complex locomotion does (Beloozerova and Sirota 2003; Liddell and Phillips 1944; Marigold and Patla 2008; Sherk and Fowler 2001; Trendelenburg 1911). During ladder locomotion cats step on the support surface with substantially less spatial variability and more accuracy compared with simple locomotion (Beloozerova et al. 2010).

Cats were habituated to the experimental environment and trained to walk in an experimental chamber over a period of 1 mo (Pryor 1975; Skinner 1938). The walking chamber was a rectangular enclosure with two connected parallel corridors (2.5 × 0.5 m each): One had a flat walking surface, and the other contained a horizontal ladder (Beloozerova and Sirota 1993a, 1993b; Beloozerova et al. 2010). The centers of the ladder crosspieces were spaced 25 cm apart, equal to one-half of a cat's average stride length during locomotion in the chamber with a flat floor. The crosspieces had flat tops and were 5 cm wide, which was slightly greater than the 3-cm-diameter support area of the cat paw. While walking in the chamber, cats passed through the two corridors sequentially, occasionally changing direction from clockwise to counterclockwise. After each round, food was dispensed into a feeding dish in one of the corners. Cats were trained, upon arrival, to stand in front of the feeding dish quietly for 3–5 s. One second in the middle of this period was considered as "standing."

Cats were accustomed to wear a cotton jacket, a light backpack with connectors, and a sock with a small metal plate on the sole of the foot for recording foot contact with the floor. The floor in the chamber and the crosspieces of the ladder were covered with an electrically conductive rubberized material. During locomotion, the duration of the swing and stance phases of the forelimb contralateral to the side of recording in the VL was monitored by measuring the electrical resistance between the plate and the floor (Steps trace in Fig. 1*C*) (Beloozerova and Sirota 1993a, 1993b; Sirota et al. 2005).

Surgical Procedures

Surgery was performed under isoflurane anesthesia in aseptic conditions. The skin and fascia were retracted from the dorsal surface of the skull. At 10 points around the circumference of the skull, stainless steel screws were implanted. The screw heads were then embedded into a plastic cast that formed a circular base. Later this base was used for fixation of connectors, electrode microdrive, and preamplifier and to rigidly hold the cat's head while searching for neurons. An arrangement of seven or nineteen 28-gauge hypodermic guide tubes was implanted above the VL. The outer diameter of the 7-tube arrangement was 1.08 mm, and that of the 19-tube arrangement was 1.8 mm. *Cat A* received the 7-tube implant in both left and right hemispheres, *cat B* received the 19-tube implant in both left and right hemispheres, and *cat C* received one 7-tube implant in the left hemisphere. The tip of the arrangement was lowered to the vertical Horsley and Clarke coordinate V +7.0. In two cats (*A* and *B*), on the left side of the head, the region of the motor cortex was exposed by removing overlaying tissues (see Fig. 5*A*). The exposure was covered with a 1-mm-thick acrylic plate. The plate was preperforated with holes of 0.36-mm diameter spaced by 0.5 mm, and the holes were filled with bone wax. The plate allowed for later implantation of stimulation electrodes in the motor cortex for identification of thalamo-cortical projection neurons.

Single-Unit Recording

Several days after the surgery the motor cortex was mapped in an awake animal with multiple-unit recording and microstimulation techniques. During microstimulation, trains of ten 25-μA, 0.2-ms cathodal pulses at 350 Hz were applied with a monopolar platinum-tungsten quartz-insulated microelectrode with impedance of 200–500 kΩ. Stimulating electrodes were implanted into the motor cortex (MC) representation of the distal (MCd) and proximal (MCp) forelimb at approximate coordinates A 25–26, L 7–9 and L 5–6, respectively (see Fig. 5, *A* and *B*). Electrodes were made of platinum-iridium Teflon-insulated wire with outer diameter of 140 μm (A-M Systems, Carlsborg, WA). The 0.4-mm tip of the wire was freed from isolation and tapered. Wires were individually inserted into the cortex 1 mm apart through perforations in the acrylic plate implanted above it and fixed.

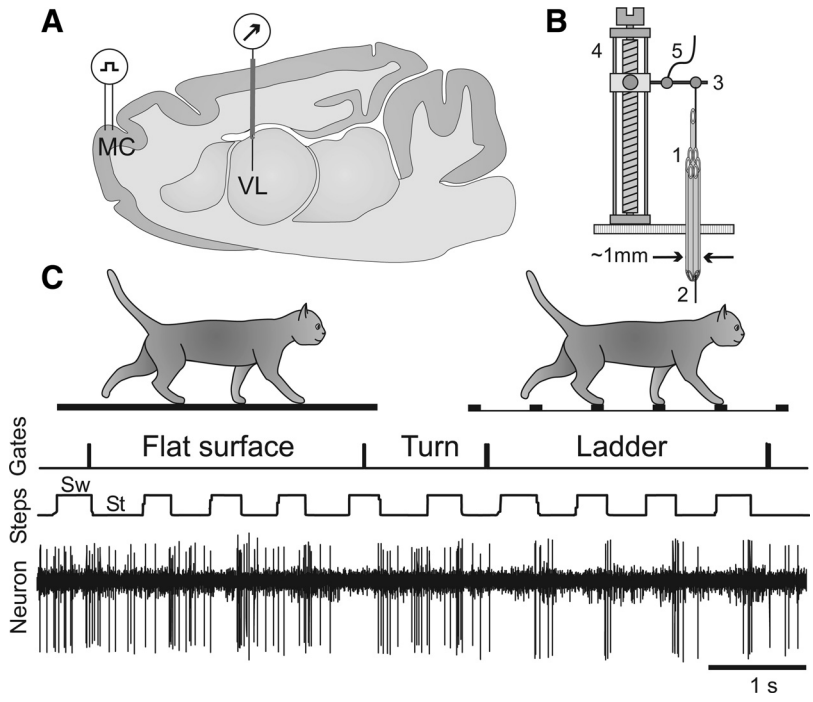

Fig. 1. Experimental paradigm. *A*: schematic drawing of a parasagittal section of the brain showing the position of chronically implanted guide tubes for recording electrodes above the ventrolateral thalamus (VL) and stimulating electrodes in the forelimb representation of the motor cortex (MC). *B*: method of insertion and advancement of electrodes into the VL. *1*: A group of 28-gauge cannulas is chronically implanted in the cortex above VL. *2*: An electrode is manually inserted into one of the cannulas and soldered to an arm (*3*) of a micromanipulator (*4*). A wire (*5*) that leads to a miniature preamplifier positioned on the head of the animal is also soldered to the arm. In this manually driven micromanipulator, 1 revolution of the screw results in 200-μm advancement of the electrode. *C*: locomotion tasks: walking in a chamber on a flat surface and along a horizontal ladder. The Gates trace indicates when the cat has passed the beginning and end of each of the chamber's corridors. The Steps trace shows the swing (Sw) and stance (St) phases of the right forelimb recorded with an electro-mechanic sensor. The Neuron trace shows discharge of a neuron from the VL.

A detailed description of the identification of the motor cortex was given earlier (Beloozerova et al. 2005).

Extracellular recordings from the VL were obtained with tungsten varnish-insulated microelectrodes (120-μm OD; FHC, Bowdoin, ME) or platinum-tungsten quartz-insulated microelectrodes (40-μm OD) pulled to a fine tip and mechanically sharpened with a diamond grinding wheel (Reitboeck 1983). The impedance of both types of electrodes was 1–3 MΩ at 1,000 Hz. A custom-made lightweight (2.5 g) manual single-axis micromanipulator chronically mounted on the cat's skull was used to advance the microelectrode (Fig. 1*B*). Signals from the microelectrode were preamplified with a miniature custom-made preamplifier positioned on the cat's head and then further amplified and filtered (0.3–10 kHz band pass) with the CyberAmp 380 (Axon Instruments, Union City, CA). After amplification, signals were digitized with a sampling frequency of 30 kHz and recorded with a computerized data acquisition package (Power-1401/Spike-2 System, Cambridge Electronic Design, Cambridge, UK) (Fig. 1*C*).

Identification of Neurons

The ventrolateral thalamus is subdivided into two parts by its afferent connections (Asanuma et al. 1983; Ilinsky and Kultas-Ilinsky 1984). The major projections to the posterior part originate in cerebellar nuclei, while the anterior part receives its primary input from the basal ganglia (Grofová and Rinvik 1974; Hendry et al. 1979; Larsen and McBride 1979; Rinvik and Grofová 1974; Sakai et al. 1996). In this study, we identify divisions of the thalamic ventrolateral nuclear complex in accordance with nuclear delineation of the cat brain atlas of Reinoso-Suarez (1961). Thus we denote the anterior division of the complex as the ventral anterior nucleus (VA). This area is analogous to the anterior part of the ventral lateral nucleus (VLa) in primates. The posterior division of the ventrolateral complex we name the ventral lateral nucleus (VL). This region is analogous to the posterior part of the primate ventral lateral nucleus (VLp). All neurons whose activity is reported in this article were collected in the VL.

The somatic receptive fields of neurons were examined in animals resting with their head restrained. Somatosensory stimulation was produced by lightly stroking fur and palpation of the muscle bellies and tendons, as well as by passive joint movements. In the left VL of two cats, *A* and *B*, in which stimulation electrodes were implanted in the left motor cortex, neurons were tested for antidromic activation from the motor cortex. The motor cortex was stimulated with 0.2-ms single rectangular pulses of 0.1- to 1.0-mA intensity applied 2–3 s apart. Current was passed between each pair of implanted wires where individual wires were within 1–1.5 mm from each other. The principal criterion for identification of antidromic activation of thalamo-cortical projection cells (TCs) was the test for collision of spikes (Bishop et al. 1962; Fuller and Schlag 1976) (see Fig. 5, *C* and *D*). For calculation of the conduction velocity, the distance between recording electrodes in the VL and stimulation electrodes in the motor cortex was estimated as 31.5 mm. Occasional orthodromic responses were not considered in this study.

Processing of Neuronal Activity

To compare the activity of neurons during two locomotion tasks we used only the strides for which the average duration in the two tasks differed by <10%. The onset of swing of the forelimb contralateral to the VL recording site was taken as the beginning of the step cycle. The duration of each step cycle was divided into 20 equal bins, and a phase histogram of the discharge rate of the neuron in the cycle was generated and averaged over all selected cycles (see, e.g., Beloozerova et al. 2010).

The coefficient of stride-related frequency modulation (M) was calculated by using a histogram of cell activity throughout the step cycle. It was defined as $M\ (\%) = (1 - F_{min}/F_{max}) \times 100$, where F_{min} and F_{max} are the minimal and the maximal frequencies of discharge in the histogram. Neurons with M > 50% were judged to be stride related. This was based on an analysis of fluctuation in the activity of neurons in the resting animal. For this analysis, the activity of 40 neurons recorded while the cat was sitting in the head-restraining device was processed as if the cat was walking. The timing of steps made by the same cat during the preceding walking test was used to construct the histogram. This analysis showed that at rest the values of M never exceed 50%. In addition to M, the "depth" of modulation (dM) was also calculated with the histogram. It was defined as $dM\ (\%) = (N_{max} - N_{min})/N \times 100$, where N_{max} and N_{min} are the number of spikes in the maximal and the minimal histogram bin, respectively, and N is the total number of spikes in the histogram.

In stride-related neurons, the portion of the cycle in which the discharge rate exceeded the value of the minimal rate plus 25% of the difference between the maximal and minimal rates in the histogram was defined as a "period of elevated firing (PEF)" (as illustrated in Fig. 6B; Sirota et al. 2005). PEFs were smoothed by renouncing all one-bin peaks and troughs (a total of 1% of bins were altered throughout the database). Using PEFs, we separated cells whose activity was concentrated in one phase of the stride from those active in different phases. In neurons with a single PEF, the "preferred phase" of discharge was assessed with circular statistics (Batshelet 1981; Drew and Doucet 1991; Fisher 1993; see also Beloozerova et al. 2003; Sirota et al. 2005).

To determine what differences in the modulation parameters of individual neurons during simple and complex locomotion could not be explained by spontaneous fluctuation in the discharge, we compared the activity of single neurons in sets of randomly selected steps of the same task. Recordings from 50 neurons that were long enough to enable selection of at least two nonoverlapping sets of 25–40 steps per task were used. From each record the first step was assigned to *set 1*, the second to *set 2*, the third to *set 3*, etc. For each neuron, the M, the dM, the preferred phase, and the duration of the PEF were calculated for each set of steps and compared. When three or more sets were available, all possible pairwise comparisons were considered; across all neurons, over 100 comparisons were made. Values of differences occurring in <5% of these "sham" comparisons across all neurons were determined. During analysis, the differences in activity characteristics of a neuron during simple and complex locomotion that exceeded these values were considered, with 95% confidence, to be caused by the difference in the locomotion tasks but not by spontaneous background fluctuation in the discharge rate.

For comparisons of activities of individual neurons in different tasks and between groups of neurons, a two-tailed *t*-test was used. A nonparametric χ^2-test was used for comparison of categorical data. For all tests, the significance level was set at $P = 0.05$. Unless indicated otherwise, for all mean values the standard deviation (SD) is given.

Histological Procedures

In *cat A*, 8 nl of 1% horseradish peroxidase-conjugated wheat germ agglutinin (WGA-HRP) (Sigma) was injected by pressure in the center of the area of recording in VL 48 h prior to the animal's death. The injection was made through a flexible capillary tube made of fused silica (147-μm OD, 50-μm ID; Polymicro Technologies, Phoenix, AZ) that was directly connected to the output of pressure microinjector PMI-200 (Dagan, Minneapolis, MN). On the day of termination the animal was deeply anesthetized with pentobarbital sodium, and reference electrolytic lesions were made in the areas of recording and stimulation. The cat was then perfused with 3% paraformaldehyde and a series of 10%, 20%, and 30% sucrose-phosphate buffer solutions (0.1 M, pH 7.4). The left half of the brain was frozen and sectioned at 40 μm in the parasagittal plane. Every fourth section was processed with a modified tetramethyl benzidine (TMB) reaction (Gibson et al. 1984; Mesulam 1982) and then lightly counterstained with thionine. Adjacent sections were stained with cresyl violet. In

addition, the right cerebellum was sectioned in the coronal plane and processed in the same manner. Brain sections were inspected under polarized light illumination. Locations of retrogradely labeled neurons were marked on digital images of brain sections with a computerized plotting system (Image Tracer, Translational Technology). Positions of electrode tracks were estimated with the use of the reference lesions.

In *cat B*, 1.5 μl of 10% red fluorescent microspheres (Lumafluor, Naples, FL) was injected into the most anterior part of the explored area in the VL 6 mo prior to the animal's death. On the day of termination, the cat was deeply anesthetized with pentobarbital sodium, and reference electrolytic lesions were made in the areas of recording and stimulation. This cat was perfused with 10% paraformaldehyde. The brain was blocked into three blocks: frontal (rostral to A14), middle (between A14 and P2), and caudal (caudal to P2). The middle block containing thalamus was sectioned in the coronal plane. The frontal cortex ipsilateral to the recorded VL and the posterior part of the brain stem with the cerebellum contralateral to the recorded VL were sectioned in the parasagittal plane. Frozen 50-μm sections were made. Every fourth section was mounted on slides, cleared with acetone and xylene, and coverslipped. Observation and digital imaging of cells retrogradely labeled with red fluorescent beads were done with Neurolucida 8, Zeiss Axioscope, and AxioCamMR3 (Carl Zeiss Int.) with a rhodamine filter. For identification of brain structures the adjacent sections were stained with cresyl violet.

Cat C received no tracers. The brain sections were obtained and stained with cresyl violet by the same techniques as in *cat B*.

RESULTS

Location of Neurons

The activity of 238 VL neurons was recorded during walking both on the flat floor and along the horizontal ladder. The majority of neurons were recorded in two cats: 94 in *cat A* and 99 in *cat B*. In *cat A*, all but 10 cells were recorded from the left VL. In *cat B*, 60 neurons were recorded from the left VL and 39 from the right VL. The remaining neurons ($n = 45$) were recorded in *cat C*.

Anatomical reconstruction. Histological examination of recording sites showed that in *cat A* recordings were obtained from the anterior portion of the VL at coordinates A 10.5–11.0, L 4.7–5.3, and V +0.5–4.0. Here and below, the vertical coordinate is given after subtraction of 10 mm from the coordinate of the atlas of Reinoso-Suarez (1961) to align it with coordinates of other commonly used atlases of the cat brain. The recording site is shown on a parasagittal section of the brain in Fig. 2*A*. It was marked with an electrolytic lesion and injection of WGA-HRP. The site is situated ~2 mm caudally to the nucleus caudatus—a landmark for identification of the anterior-posterior position of the section. A reconstruction of the locations of neurons that were recorded in this cat is given in Fig. 2*D*, *plates 11.0–10.5*.

In *cat B*, nearly symmetrically on the left and right sides of the thalamus, recorded cells were located in the central portion of the VL at coordinates A 9.5–10.75, L/R 3.0–5.0, and V −0.5 to +3.5. The recording site in the left thalamus is shown on a coronal section in Fig. 2*B*. It was labeled with an electrolytic lesion and injection of red fluorescent beads (see Fig. 4*A*). A landmark for identification of the anterior-posterior position of the section was the caudal putamen, which at this level has a striped appearance in the cat. A reconstruction of locations of neurons, combined from the left and right VL, is shown in Fig. 2*D*, *plates 10.75–9.5*.

In *cat C*, recordings were made from the most caudal aspect of the VL at coordinates A 8.75–9.25, L 4.0–4.3, and V 0.5–1.5. A reference lesion that was made ~200 μm caudally to the most caudal recording track in this cat is shown on a coronal section of the thalamus in Fig. 2*C*. A landmark for identification of the anterior-posterior position of the section was the most rostral aspect of the lateral geniculate body (LG) that is visible in this section. A reconstruction of locations of neurons recorded in this cat is given in Fig. 2*D*, *plates 9.25–8.75*.

Receptive fields. The somatosensory receptive fields of 168 neurons were tested. All receptive fields were found on the contralateral side of the body. One-third of neurons (32%, 53/168) responded to passive movements of the shoulder joint and/or palpation of muscles on the back or neck. Slightly more than half of these cells showed directional preference to shoulder movement and responded better either to flexion (17/168) or to extension and/or abduction of the joint (13/168). Eighty-four percent of shoulder-related cells were TCs. Fewer neurons (18%, 30/168) responded to movements in the elbow joint. Almost all of these neurons had a directional preference: half of them responded to flexion and another half to extension of the elbow. Ninety-five percent of tested cells were TCs. The number of neurons with receptive fields on the paw or wrist was relatively small (10%, 17/168). Typically, these neurons responded to pressure on the paw or to the wrist ventral flexion. Sixty-seven percent of tested cells were TCs. In addition, 15% (25/168) of neurons responded to stimulation of most of the forelimb, typically to flexion in the shoulder and extension in the elbow, or to synergistic movements in both joints. This group also included the only two neurons which activity diminished during somatosensory stimulation. Among all cells tested only one had a cutaneous receptive field responding to brushing of fur on the medial surface of the paw. We found only six cells that had somatosensory receptive fields on the hindlimb. Overall, characteristics of somatosensory receptive fields were in agreement with previously reported data (e.g., Asanuma and Hunsperger 1975).

Neurons that responded to stimulation of different parts of the forelimb were distributed randomly in the VL: there were no clear clusters of shoulder-, elbow- or wrist-related cells (Fig. 2*D*). There were also 23% (38/168) of neurons that did not respond to any somatosensory stimulation. They were intermingled with the responsive cells. Five of these cells responded to vestibular stimulation produced by the whole animal translations or rotations; they were found laterally and caudally in the VL (Fig. 2*D*). Two other neurons without somatosensory receptive fields responded to visual stimulation.

Afferent connections. In *cat A*, WGA-HRP was injected in the center of the area of recordings. The injection had a core ~1.5 mm in diameter (dark area in Fig. 2*A*). Numerous retrogradely labeled neurons were found in the anterior half of the lateral (dentate) nucleus and in the anterior interposed nucleus of the right (contralateral) cerebellum (Fig. 3*A*). In the dentate nucleus, labeled cells were found in its rostral part, with the highest density at P 8.0–8.5, and were not seen caudal to P 9.0. The most ventral part of the nucleus was free from labeled cells. In the anterior interposed nucleus, labeled neurons filled its entire rostro-caudal extent but were confined to the lateral half of the nucleus. Ipsilaterally to the injection site, labeled neurons were found in the lateral half of the entopeduncular nucleus (from L 7.0 to L 5.5).

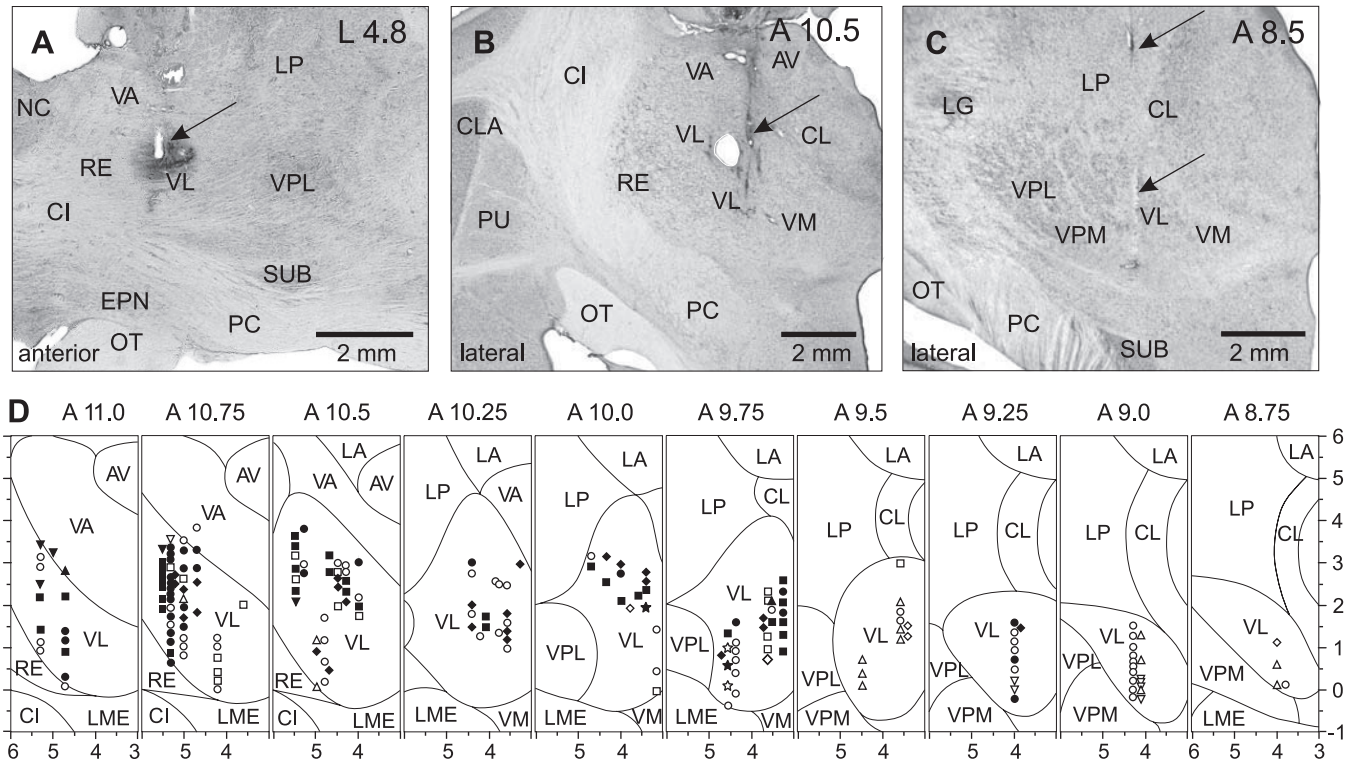

Fig. 2. Sites of recording in the VL. *A*: recording site in *cat A* is shown on a photomicrograph of a parasagittal section of the thalamus. It was located in the rostral VL. Arrow points to the electrolytic lesion mark and the darkened area of tissue filled with horseradish peroxidase-conjugated wheat germ agglutinin (WGA-HRP). The site is ~2 mm caudally to the nucleus caudatus (NC) of the basal ganglia. *B*: recording site in *cat B* is shown on a photomicrograph of a coronal section of the thalamus. It was positioned in the middle of the VL. Arrow points to the electrolytic lesion mark and the darkened area where fluorescent beads were deposited. The caudal part of putamen (PU), a landmark for the anterior-posterior position of the section, is seen laterally. *C*: recording site in *cat C* is shown on a photomicrograph of a coronal section of the thalamus. It was positioned in the caudal VL. Arrows point to a track from a reference electrode. The most rostral aspect of the lateral geniculate body (LG), a landmark for the anterior-posterior position of the section, is visible laterally. *D*: reconstruction of positions of individual neurons recorded during locomotion in *cats A*, *B*, and *C*. Squares, neurons with somatosensory receptive fields on the shoulder (responding to passive movements in the shoulder joint and/or palpation of muscles on the back or neck); diamonds, cells that were activated by movements in the elbow; up-facing triangles, neurons with receptive fields on the wrist or paw; down-facing triangles, neurons whose receptive field encompassed the entire forelimb; stars, neurons responsive to vestibular stimulation; circles, neurons without somatosensory receptive fields and those whose receptive fields were not identified. Filled symbols represent neurons with axonal projections to the motor cortex (thalamo-cortical neurons, TCs); open symbols represent neurons whose projections were not identified. AV, nucleus anterio-ventralis thalami; CI, capsula interna; CL, nucleus centralis lateralis; CLA, claustrum; EPN, nucleus entopeduncularis; LA, nucleus lateralis anterior; LME, lamina medullaris externa thalami; LP, nucleus lateralis posterior; OT, optic tract; PC, pedunculus cerebri; RE, nucleus reticularis thalami; SUB, nucleus subthalamicus; VA, nucleus ventralis anterior; VL, nucleus ventralis lateralis; VM, nucleus medialis; VPL, nucleus ventralis postero-lateralis; VPM, nucleus ventralis postero-medialis.

Most laterally, labeled cells filled the entire nucleus, but more medially cells were concentrated only in the anterior and posterior poles of it.

In *cat B*, red fluorescent beads were injected into the most anterior part of the explored area. Injected beads spread vertically by ~3 mm and filled the entire dorso-ventral extent of the VL; medio-laterally, they covered 0.6–0.7 mm of the medial part of the nucleus (L 3.5–4.2; Fig. 4*A*). Labeled cells were found throughout the entire rostro-caudal extent of the contralateral dentate nucleus (Fig. 3*B*). In the lateral half of the nucleus labeled cells were located mostly ventrally; in the medial half they were also present more dorsally, where two clusters of cells were evident: the rostral and caudal clusters (Fig. 4*D*). Labeled cells were also found in the contralateral posterior interposed nucleus. They were distributed throughout its entire rostro-caudal extent, most intensively at the laterality of L 3.0–4.0 mm (Fig. 3*C* and Fig. 4*E*). A number of labeled neurons were seen in the contralateral anterior interposed nucleus (Fig. 3*C*). Also, several cells were found throughout the contralateral fastigial nucleus (not shown), and a few were seen in the contralateral inferior vestibular nucleus (Fig. 3*C* and Fig. 4*G*). In addition, a longitudinally extended group of labeled cells was found in the contralateral dorsal hypothalamic area. The ipsilateral entopeduncular nucleus was free from label. Numerous labeled cells were found in the ipsilateral frontal cortex, throughout layer VI of the anterior and posterior sigmoid gyri, at the laterality of L 4.0–9.0 (Fig. 4*H*), as well as more caudally, across the lateral ansate sulcus into suprasylvian gyrus up to caudal area 5 (Fig. 4*I*). In area 4γ, labeled cells densely filled the entire layer VI. In other cortical areas labeled cells were sparser and formed a thinner stretch through layer VI (Fig. 4*C*). In all cortical areas that contained labeled neurons in layer VI, medium-size labeled pyramidal cells were occasionally found also in the adjacent part of layer V.

Neurons Projecting to the Motor Cortex

Among the 238 neurons that were recorded during locomotion, 116 were identified as projecting to the motor cortex [thalamo-cortical neurons (TCs)]. Positions of stimulating electrodes in the left precruciate cortex of *cat B* are schematically shown in Fig. 5*A*. The electrodes were placed in the distal forelimb (paw) representation of the motor cortex (MCd) and in the proximal forelimb

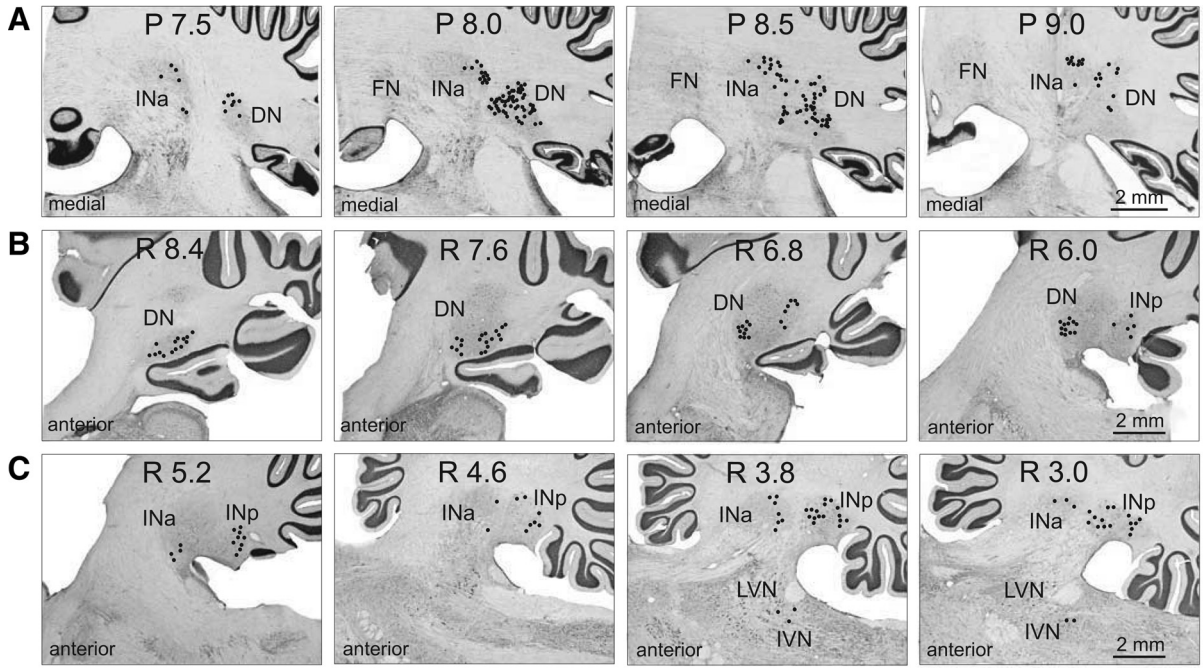

Fig. 3. Cerebellar projections to the recording area in the VL. *A*: neurons in the anterior interposed (INa) and lateral (dentate, DN) nuclei in *cat A*, retrogradely labeled with WGA-HRP. Neurons are depicted with black circles on photomicrographs of coronal sections of the cerebellum contralateral to the injection site. *B* and *C*: neurons in the dentate, anterior, and posterior (INp) interposed nuclei and inferior vestibular nucleus (IVN) in *cat B*, retrogradely labeled with red fluorescent beads. Neurons are shown on photomicrographs of parasagittal sections of the cerebellum contralateral to the injection site. Each circle represents 1 labeled neuron. LVN, lateral vestibular nucleus.

(elbow, shoulder) representation (MCp) (see METHODS). In Fig. 5*B*, a track and an electrolytic lesion made by one of the stimulation electrodes are shown on a photomicrograph. The lesion is visible in the cortical layer VI adjacent to layer V that is populated with giant pyramidal cells characteristic for area 4γ. In both *cat A* and *cat B*, all stimulating electrodes were placed in layer VI of area 4γ in the precruciate sigmoid gyrus. An example of an antidromic response of a TC neuron to stimulation of MCd is given in Fig. 5, *C* and *D*.

The TCs were distributed fairly evenly throughout the area of recording. In Fig. 2*D*, they are represented by filled shapes. Most TC neurons responded to stimulation of either MCd or MCp, and only a few responded to stimulation of both sites. Interestingly, the vast majority (72%) of neurons

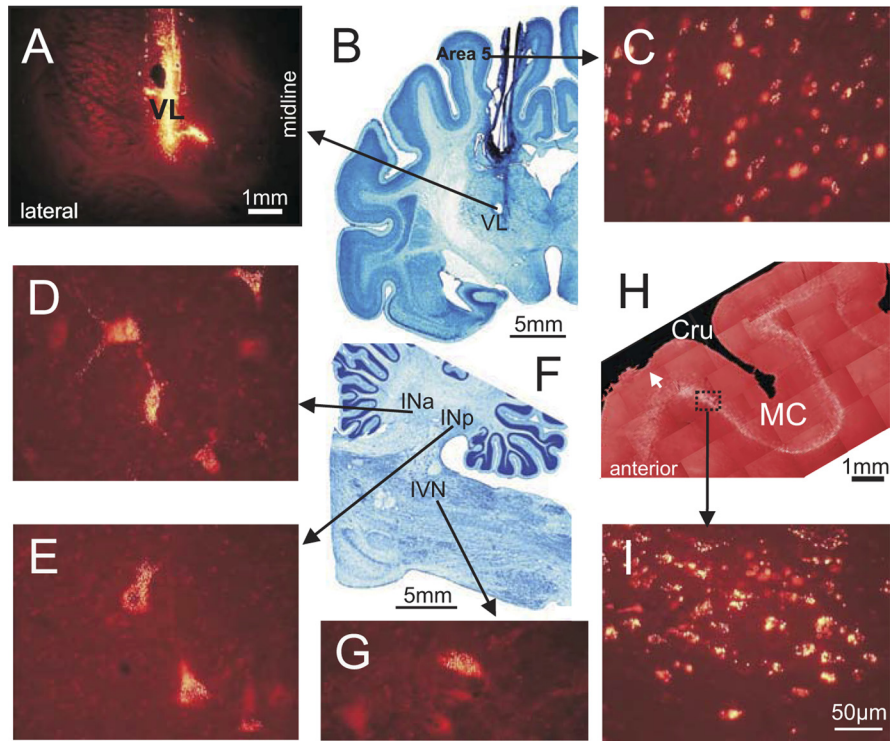

Fig. 4. Cerebellar and cortical neurons labeled with fluorescent beads in *cat B*. *A*: coronal section of the thalamus containing the electrolytic lesion mark and fluorescent bead deposit site in the area of recording as seen with a rhodamine filter. *B*: coronal section of the brain at the same anterior-posterior level as in *A*, cresyl violet stain. *C*: labeled neurons in the caudal area 5 in the suprasylvian gyrus. *D*: labeled neurons in the anterior interposed nucleus (INa). *E*: labeled neurons in the posterior interposed nucleus (INp). *F*: parasagittal section of the brain stem and cerebellum, cresyl violet stain. *G*: labeled neurons in the inferior vestibular nucleus (IVN). *H*: composition of parasagittal sections of the frontal cortex showing the fold of cruciate sulcus (Cru). Sections contain neurons in layer VI labeled with red fluorescent beads. White arrow points to a small depression on the top of the cortex that was left by one of the stimulation electrodes chronically implanted in the motor cortex (MC). *I*: labeled neurons in the forelimb representation of the motor cortex in the anterior sigmoideus gyrus. In *C*, *D*, *E*, and *G* the scale is as in *I*.

projecting to MCd had receptive fields on proximal parts of the forelimb, shoulder, or elbow, and only 9% had receptive fields on the wrist or paw. Neurons projecting to the more medial cortical areas that are related to elbow and shoulder, MCp, had various receptive fields. Latencies of antidromic responses of different TCs varied in the range of 0.5–5.5 ms (Fig. 5*E*). Estimated conduction velocities ranged from 5 to 70 m/s (Fig. 5*F*). We have arbitrarily divided the TC neurons into two subgroups: responding with a latent period of 1.0 ms or faster ("fast" TCs) and responding with longer delays ("slow" TCs). Two-thirds of slow TCs were collected in *cat A*.

Activity During Standing

The discharge rate of VL neurons during standing varied in the range of 0.6–63 spikes/s and was 20.2 ± 12.5 spikes/s on average. Neurons with somatosensory receptive fields were more active than neurons without them [24.3 ± 1.5 vs. 15.4 ± 2.1 spikes/s (means ± SE), respectively; $P < 0.05$, *t*-test]. Neurons located laterally with coordinates L 4.5–5.3 (mostly collected from *cat A*; Fig. 2, *A* and *D*) were less active than those located medially at L 3.1–4.4 (mostly collected from *cat B*; Fig. 2, *B* and *D*) [14.8 ± 1.2 vs. 25.6 ± 1.9 spikes/s (means ± SE); $P < 0.05$, *t*-test]. Fast-conducting TCs were more active on average than slow-conducting TCs [23.7 ± 2.2 vs. 15.4 ± 1.2 spikes/s (means ± SE); $P < 0.05$, *t*-test; Fig. 5*G*]. Moreover, there was a linear relationship between conduction velocity and the discharge rate in the standing animal (Fig. 5*H*).

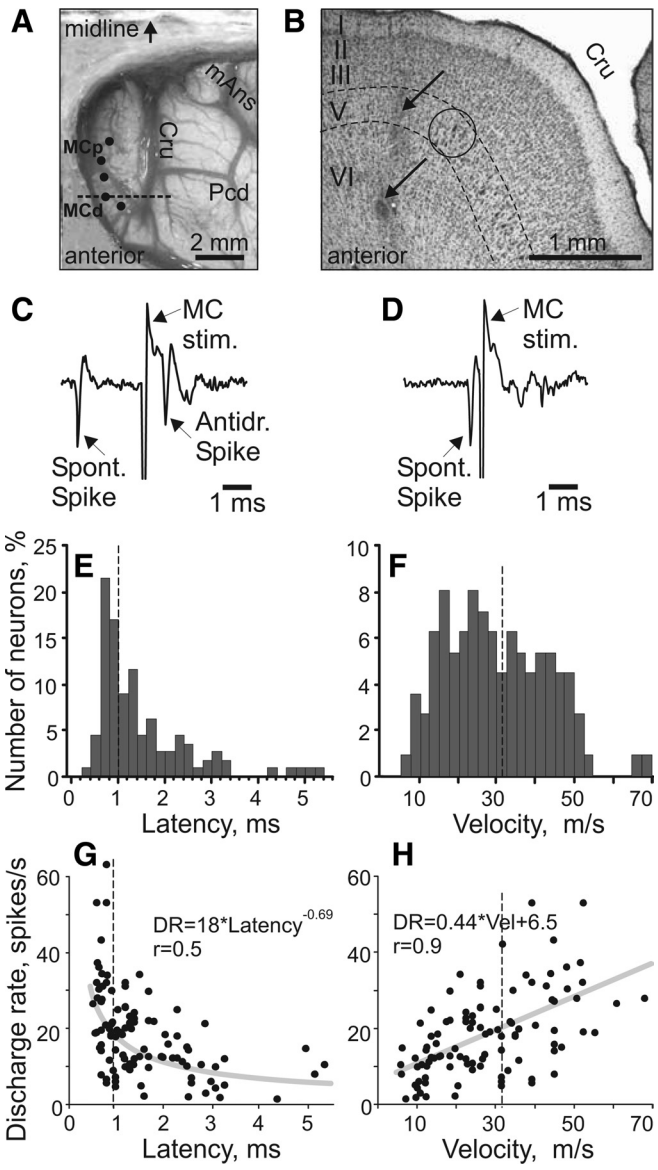

Fig. 5. Axonal conduction velocities of thalamo-cortical projection neurons (TCs). *A*: photograph of the dorsal surface of the left frontal cortex of *cat B*. Entrance points of stimulation electrodes into the precruciate sulcus are schematically shown by black dots. Electrodes were placed in the paw (the motor cortex distal forelimb representation, MCd) and the elbow and shoulder (the motor cortex proximal forelimb representation, MCp) as determined by multiunit recording and microstimulation procedures. The position of the parasagittal section, whose photomicrograph is shown in *B*, is indicated by a dashed line. Cru, cruciate sulcus; Pcd, postcruciate dimple; mAns, medial ansate sulcus. *B*: photomicrograph of a parasagittal section through the rostral precruciate gyrus stained with cresyl violet. Layers of cortex are numbered. Layer V, which contains giant pyramidal cells, is highlighted by dashed lines. One of the clusters of giant cells in layer V that are characteristic for area 4γ is circled. Arrows point to a track and an electrolytic lesion made by a stimulation electrode that was placed in layer VI. *C*: stimulation of the motor cortex evoked a spike in a TC neuron with a latency of 0.8 ms. *D*: to determine whether this spike was elicited antidromically, on the next trial a spontaneous spike of the neuron was used to trigger cortical stimulation with 0.4-ms delay. Stimulation delivered with a delay smaller than the time needed for a spontaneous spike to reach the site of stimulation (that is, approximately equal to the latent time of an antidromic spike) was not followed by a response. This indicated a collision of ortho- and antidromically conducted spikes and confirmed the antidromic nature of the evoked spike. *E*: distribution of latencies of antidromic responses to stimulation of the motor cortex of all 116 TC neurons whose activity was recorded during locomotion. *F*: distribution of estimated conduction velocities. In *E* and *F* dashed lines separate "fast" (latencies 0.4–1.0 ms)- and "slow" (latencies 1.1–6.0 ms)-conducting neurons. *G*: relationship between the mean discharge rate of individual neurons in the resting animal and their antidromic latency, approximated with a power function. *H*: relationship between the mean discharge rate of individual neurons in the resting animal and axonal conduction velocity, approximated with a linear regression. *r*, Coefficient of correlation.

Characteristics of Locomotion

During recording from each neuron, cats ran between 15 and 100 (typically 25–50) times down each of the corridors. From these trials, 15–150 strides (50 ± 30) of each locomotion task were selected for the analysis according to criteria outlined in METHODS. For different neurons, the average duration of selected strides was between 600 and 750 ms. The ratio of stance duration to the duration of the cycle (the stride duty factor) was 0.57–0.60. The gait that cats used during walking on both the flat surface and along the ladder was a walk with the support formula 2-3-2-3-2-3-2-3 (Hildebrand 1965). Further details of biomechanics and muscle activities in cats walking on the flat surface and along the horizontal ladder in this experimental setup can be found in Beloozerova et al. (2010).

Population Activity During Simple and Complex Locomotion

Upon transition from standing to walking the discharge rate of many neurons changed. It increased, up to 10-fold, in 31% of neurons or decreased, down to less than one-half, in 27% of them. Because changes in the activity were opposite in different neurons, the average discharge rate of the whole population did not change. We found no correlation between receptive fields of the neurons and changes in the discharge rate with the

start of locomotion. The average activity of neurons without somatosensory receptive fields, however, was lower than that of somatosensory responsive cells ($P < 0.05$, *t*-test). Neurons with receptive fields on different parts of the forelimb had similar average activity. The average discharge rate of neurons during walking along the horizontal ladder was similar to that observed during standing and walking on the flat surface. Fast-conducting TCs were more active than slow-conducting TCs during all tasks, however ($P < 0.05$, *t*-test).

During simple locomotion, the activity of 92% of neurons (220/238), including 91% of TCs (105/116), was modulated in the rhythm of strides: it increased in one phase of the stride and decreased in another phase. Two basic patterns of modulation were recognized: one or two PEFs (see METHODS). Most common was the one-PEF pattern seen in 67% (148/220) of neurons, including 63% (66/105) TCs. Two PEFs were observed in 31% (69/220) of cells, including 35% (37/105) TCs. During locomotion along the ladder, the activity of 96% of neurons (229/238) was also modulated: the one-PEF pattern was seen in 63% (145/229) of neurons and the two-PEF pattern in 34% (78/229) of neurons. In addition, there were three neurons with three PEFs during simple locomotion and seven such neurons during ladder locomotion; we did not consider activity of these cells further. Most neurons had a similar modulation pattern during both locomotor tasks, but in some neurons the pattern changed. We will first compare activities of one- and two-PEF populations during simple and complex locomotion and then look into activities of individual cells.

Neurons with one PEF per stride. During simple locomotion a representative neuron shown in Fig. 6 discharged throughout all phases of the stride except for the middle of stance, when it was practically silent (Fig. 6, *A* and *B*). The discharge within the PEF varied in intensity, forming three small subpeaks; the maximum discharge rate was 80 spikes/s. In Fig. 6*B* the PEF is indicated by a solid black horizontal line, and the preferred phase of the activity is shown by a circle. During ladder locomotion, rather than discharging throughout most of the stride cycle, the neuron was active almost exclusively around the swing-stance transition (Fig. 6, *G* and *H*) but peaked near the same preferred phase as during simple locomotion. Its firing rate reached 118 spikes/s, significantly higher than during simple locomotion ($P < 0.05$, *t*-test), whereas the activity in the trough during stance remained low. Consequently, the strength of modulation was larger during ladder than during simple locomotion. The duration of the PEF shortened by one-half.

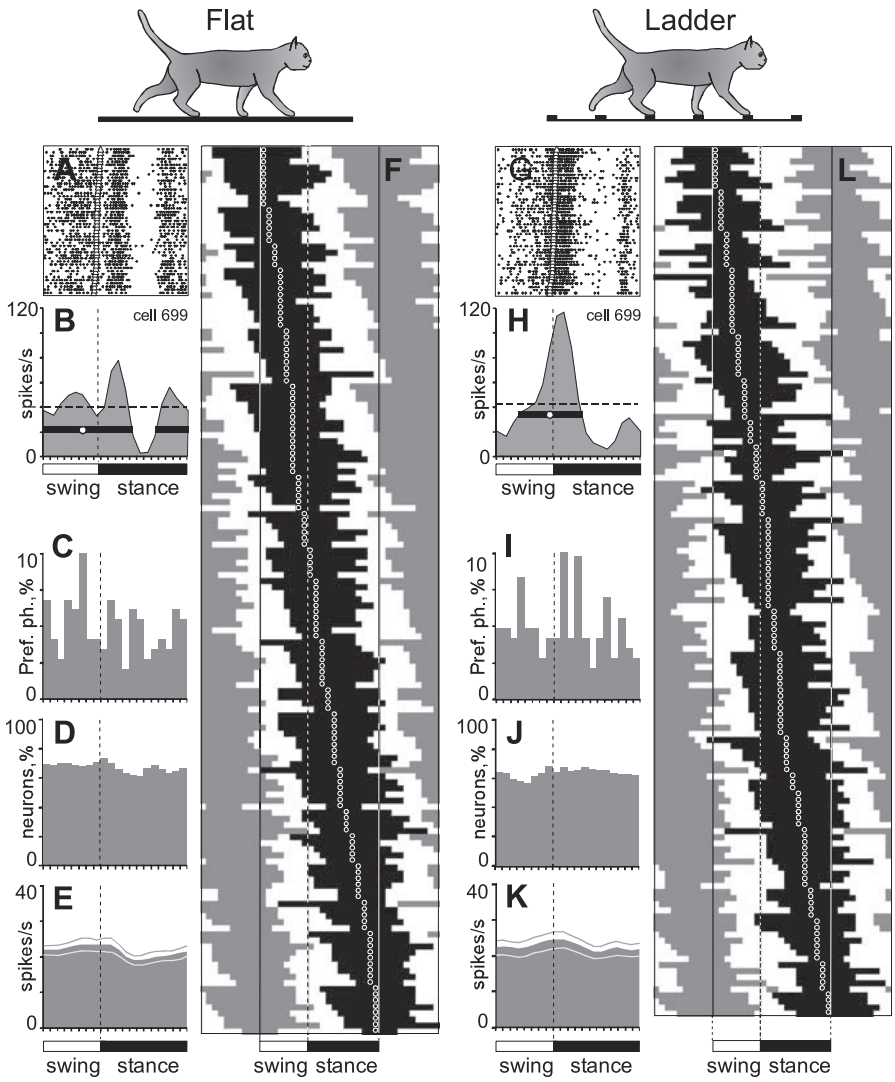

Fig. 6. Population characteristics of one-period of elevated firing (PEF) neurons. *A* and *B* and *G* and *H*: example of activity of a typical neuron (*group I* neuron, see Fig. 13) during walking on the flat surface (*A*, *B*) and along the horizontal ladder (*G*, *H*). The activity is presented as a raster of 50 step cycles (*A*, *G*) and a histogram (*B*, *H*). In the rasters, the duration of strides is normalized to 100%, and the rasters are rank ordered according to the duration of the swing phase. The end of swing and the beginning of the stance in each cycle is indicated by an open triangle. In histograms, the horizontal interrupted line indicates the average discharge frequency during standing. The horizontal black bar shows the PEF, and the circle indicates the preferred phase (as defined in METHODS). *C* and *I*: distribution of preferred phases of activity of all one-PEF neurons during simple (*C*) and ladder (*I*) locomotion. *D* and *J*: proportion of active neurons (neurons in their PEF) in different phases of the step cycle during simple (*D*) and ladder (*J*) locomotion. *E* and *K*: mean discharge rate of neurons during simple (*E*) and ladder (*K*) locomotion. Thin lines show SE. *F* and *L*: phase distribution of PEFs during simple (*F*) and ladder (*L*) locomotion. Each horizontal bar represents the PEF location of 1 neuron (shown in black in 1 cycle only) relative to the step cycle. Neurons are rank ordered so that those active earlier in the cycle are plotted at *top* of graph. Vertical solid lines highlight 1 cycle. Vertical interrupted lines denote end of swing and beginning of stance phase.

Figure 6, *F* and *L*, show phase positions within the step cycle of PEFs and preferred phases of all neurons during simple and ladder locomotion, respectively. One can see that, during both tasks, PEFs of different neurons were distributed fairly evenly over the cycle. Duration of PEFs differed between neurons in the range of 20–90% of the cycle and lasted ~65% of the cycle on average during either task. In the vast majority of neurons, the discharge rate within the PEF varied. In 27% of neurons at least two subpeaks with activity above the average discharge rate were observed; this level is twice as high as the threshold discharge rate for PEF recognition. The strength of the stride-related modulation of the discharge varied between neurons. About 20% of neurons were completely silent for a part of the step cycle; the majority, however, were active throughout the cycle, while their discharge rate was modulated. During simple locomotion, the coefficient of modulation, M, was 81 ± 1%, and the coefficient dM was 8 ± 0.2%. During ladder locomotion the strength of modulation was larger: M was 87 ± 1%, and dM was 9.6 ± 0.3% (means ± SE); the increase in both M and dM was highly significant ($P < 0.0001$, *t*-test). Because of an even distribution of PEFs throughout the cycle and their relatively long duration, however, PEFs overlapped each other, and 60–70% of neurons were simultaneously active at any time of the cycle during either task (Fig. 6, *D* and *J*). As a result, despite the substantial modulation of the activity in most of the individual neurons, the averaged discharge rate of the population was around 20–25 spikes/s throughout the cycle during both simple and ladder locomotion (Fig. 6, *E* and *K*).

We did not find any simple correlation between neuronal responses to somatosensory stimulation in the quiescent animal and preferred phases of their activity during locomotion. During simple locomotion, the preferred phases of most neurons responsive to passive extension of the shoulder or elbow were timed to the periods of extension of the shoulder or elbow, respectively. In contrast, most neurons responsive to passive flexion of the shoulder or ventral flexion of the wrist had preferred phases not timed to periods of flexion in these joints. Furthermore, an overwhelming majority of neurons without somatosensory receptive fields had profoundly modulated activity. Similar inconsistency was found during ladder locomotion.

In contrast to this inconsistency, neurons with receptive fields involving different joints tended to have their PEF in specific phases of the step cycle (Fig. 7). During simple locomotion, neurons responsive to passive movements in the shoulder joint and/or palpation of back, chest, or neck muscles more often had PEF during the swing and early stance phases (Fig. 7*A*). During ladder locomotion, however, these neurons more often had their PEF during stance, and their population activity during stance was higher than that during simple locomotion (Fig. 7*D*). Neurons responsive to passive movement of the elbow more often had their PEF in the late stance and early swing during both tasks (Fig. 7, *B* and *E*). Most neurons responsive to stimulation of the paw or movement in the wrist joint had their PEF in the beginning and middle of stance (Fig. 7, *C* and *F*). PEFs and preferred phases of neurons without receptive fields were evenly distributed over the cycle.

The one-PEF neurons were distributed over the entire area of recording in the VL without apparent clustering; they projected to both distal and proximal forelimb representations in the motor cortex via both fast- and slow-conducting TCs. When grouped according to the site of projection in the motor cortex (distal vs. proximal), or the conduction velocity (fast vs. slow), during simple locomotion the neuronal populations did not

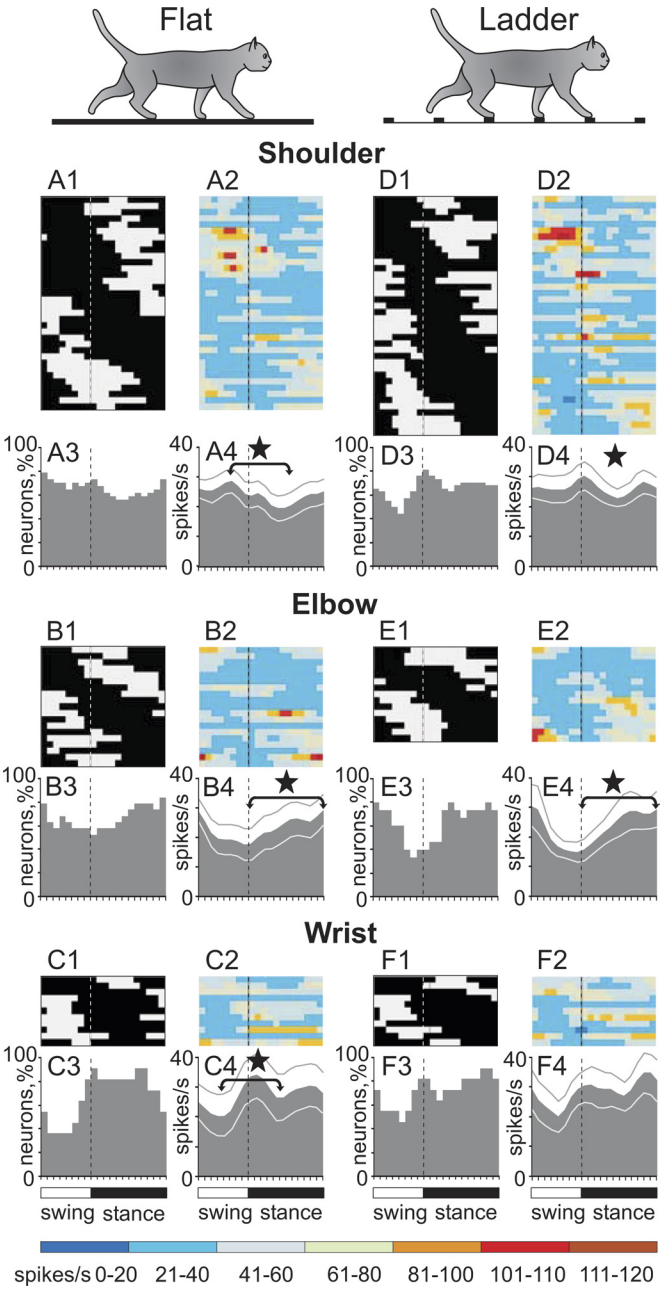

Fig. 7. One-PEF neurons with receptive fields on different joints tend to discharge during different phases of the stride. *A* and *D*: activity of neurons responsive to movements in the shoulder joint and/or palpation of back, chest, or neck muscles during simple (*A*) and ladder (*D*) locomotion. *A1* and *D1*: phase distribution of PEFs. *A2* and *D2*: corresponding phase distribution of discharge frequencies. Average discharge frequency in each 1/20th portion of the cycle is color-coded according to the scale shown at *bottom*. *A3* and *D3*: proportion of active neurons (neurons in their PEFs) in different phases of the step cycle during simple (*A3*) and ladder (*D3*) locomotion. *A4* and *D4*: mean discharge rate during simple (*A4*) and ladder (*D4*) locomotion. Thin lines show SE. Vertical interrupted lines denote end of swing and beginning of stance phase. *B* and *E*: activity of neurons responsive to passive movement of the elbow joint. *C* and *F*: activity of neurons responsive to stimulation of the paw or movement in the wrist joint. ★Significant differences between the activity of populations during different periods of the cycle.

show any differences in the strength of modulation or duration of PEF. However, the neurons projecting to the cortical paw representation, as well as slow-conducting TCs, had subtle but statistically significant higher activity during swing compared with stance, while their counterparts did not. Furthermore, the neurons with preferred phases in the first half of swing (SW1) or in the first half of stance (ST1) had higher activity during their respective preferred periods, compared with the neurons with preferred phases in the second half of swing (SW2) or in the second half of stance (ST2) [36.8 ± 2.2 vs. 27.3 ± 1.5 spikes/s (means ± SE); $P < 0.05$, *t*-test].

During ladder locomotion, fast TCs were more active during swing compared with stance ($P < 0.05$, *t*-test), whereas slow TCs tended to be more active in the opposite phase. The step-related modulation of neurons with shoulder or elbow receptive fields was stronger than that of neurons with wrist/paw receptive fields: The coefficient M was 87–90% vs. 75%, and dM was 9.4–9.8% vs. 6.4% ($P < 0.005$, *t*-test). In addition, neurons with preferred phases in the first half of swing (SW1) became still more active during swing ($P < 0.05$, *t*-test), while the activity of neurons with preferred phases in the second half of swing (SW2) did not change, and their number decreased by 35%.

Neurons with two PEFs per stride. An example of activity of a representative neuron with two PEFs is shown in Fig. 8. During simple locomotion this neuron was active during both swing-stance and stance-swing transitions (Fig. 8*A*). The discharge rate reached 25 and 30 spikes/s in two different peaks (Fig. 8*B*). On the ladder, the neuron was still active during swing-stance and stance-swing transitions, but its two PEFs deviated from each other in both amplitude and duration. The PEF during swing-stance transition became markedly longer and had higher discharge rate than the other PEF. In addition, one of the troughs deepened. As a result, the strength of modulation was larger during ladder locomotion, while the total duration of PEFs was shorter.

Figure 8, *E* and *J*, show the distributions of PEFs in all two-PEF neurons. By the phase and duration of their PEFs, neurons could be loosely subdivided into three groups. The first group included cells that had a long PEF during swing and a short PEF during stance—the "swing" neurons (33% of cells). PEFs of these neurons are concentrated in the upper third of the graphs. The second group consisted of cells that had a long PEF during stance and a short PEF during swing—the "stance" neurons (25% of cells). PEFs of these neurons are concentrated in the lower part of the graphs. In both swing and stance neurons, during simple locomotion the longer PEF was typically (in 70% of cells) also the stronger one, as the discharge rate in it exceeded that in the shorter PEF by 20 ± 15 spikes/s. The duration of the longer PEF ranged from 25% to 70% of the cycle, and the duration of the shorter PEF ranged from 10% to 30%. During ladder locomotion, the activity of stance neurons differed in the discharge intensity during swing: in many of these neurons the discharge rate during the shorter PEF in swing was as high as during the longer PEF in stance. By contrast, in the majority (73%) of swing neurons during ladder locomotion the activity during the longer PEF in swing was still higher.

The third and most populous group included neurons whose two PEFs were of approximately similar duration, ranging from 15% to 40% of the cycle each (40% of cells). In these "transition" neurons, the first PEF typically started in mid-swing and lasted into stance, while the second PEF started in midstance and continued into swing. In Fig. 8, *E* and *J*, PEFs of these neurons are concentrated in the middle of the graphs. The average duration of each PEF was 30 ± 7% of the step cycle, approximately half as long as in the one-PEF group. Although in transition neurons the two PEFs were of a similar duration, in 68% of them the discharge in one of the PEFs was more intense, by 15 ± 12 spikes/s on average.

Because of a rather even distribution of PEFs of different neurons throughout the cycle, and their long duration, the PEFs

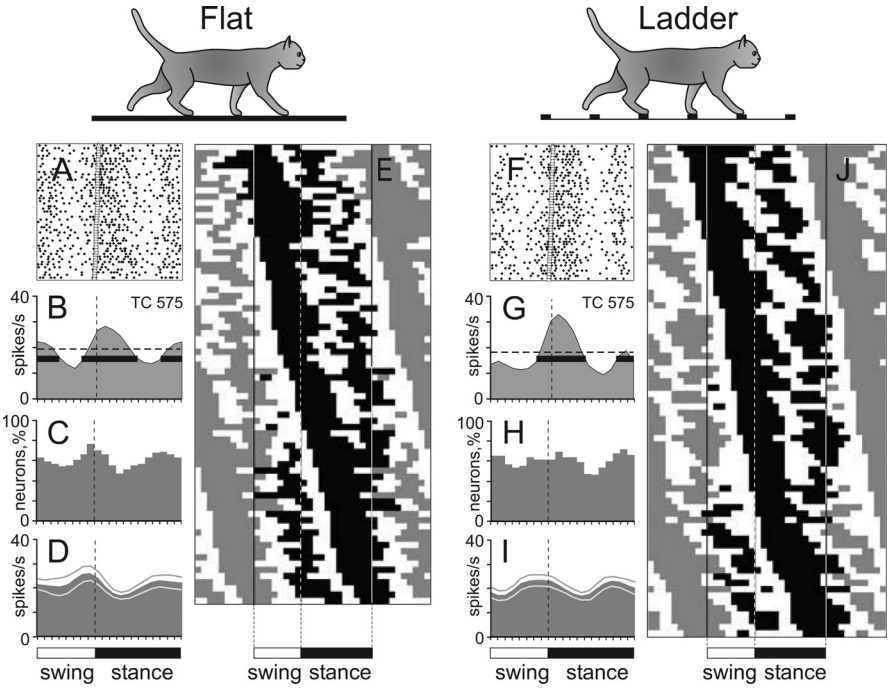

Fig. 8. Population characteristics of two-PEF neurons. *A* and *B* and *F* and *G*: example activity of a typical neuron (*group II* neuron, see Fig. 13) during walking on the flat surface (*A*, *B*) and along the horizontal ladder (*F*, *G*). Activity is presented as a raster of 50 step cycles (*A*, *F*) and as a histogram (*B*, *G*). In rasters, the end of swing and the beginning of the stance phase in each cycle is indicated by an open triangle. In histograms, the horizontal interrupted line indicates the average discharge frequency during standing; the horizontal black bar shows PEFs. *C* and *H*: proportion of active neurons (neurons in their PEF) at different phases of step cycle during simple (*C*) and ladder (*H*) locomotion. *D* and *I*: mean discharge rate during simple (*D*) and ladder (*I*) locomotion. Thin lines show SE. *E* and *J*: phase distribution of PEFs during simple (*E*) and ladder (*J*) locomotion. Each trace shows PEFs of 1 neuron (shown in black in 1 cycle only). Vertical solid lines highlight 1 cycle. Vertical interrupted lines denote the end of swing and beginning of stance phase.

overlapped each other, and 50–70% of neurons were simultaneously active in any phase of the cycle (Fig. 8, *C* and *H*). The discharge rate of the population of two-PEF neurons was slightly modulated around the value of 20 spikes/s, with two small peaks during the swing-stance and stance-swing transition periods (Fig. 8, *D* and *I*).

During simple locomotion, the strength of stride-related frequency modulation, M, was 79 ± 12% and dM was 8.2 ± 3.4%. Both values were similar to those in the one-PEF group. Upon transition to ladder locomotion, however, in sharp contrast with the one-PEF group, the strength of modulation in the two-PEF population did not increase.

In two-PEF cells the active phase during locomotion usually differed from the phase that could be expected based on somatosensory responses in the resting animal, similar to that in one-PEF neurons. Unlike one-PEF neurons, however, the activities of two-PEF cells with receptive fields involving different joints were similarly distributed across the stride: all groups had two subtle maxima at swing-stance and stance-swing transitions.

Two-PEF neurons were distributed over the entire area of sampling in the VL and intermingled with one-PEF cells. Both fast- and slow-conducting TCs with two PEFs projected to both the distal and proximal forelimb representations in the motor cortex. Groups of neurons assembled according either to the site of projection to the motor cortex (distal vs. proximal) or to conduction velocity (fast vs. slow) during simple locomotion were similar in their activity phases, strength of modulation, and duration of PEFs. During ladder locomotion, however, the step-related modulation of neurons projecting to the paw area was stronger than that of neurons projecting to the elbow or shoulder areas: the coefficient M was 84 ± 2% vs. 77 ± 3%, and dM was 9.3 ± 0.6% vs. 7.0 ± 0.7% (mean ± SE) ($P < 0.05$, *t*-test). Also, the PEFs of neurons projecting to the paw/wrist area were slightly shorter, lasting for 55 ± 2% rather than 65 ± 3% of the cycle ($P < 0.05$, *t*-test). During either task, swing, stance, and transition neurons were similar in their average and peak discharge rates, strength of modulation, and durations of PEF. Swing neurons, however, were more active during swing than stance neurons during stance (30 ± 2.7 vs. 20 ± 1.2 spikes/s; $P < 0.05$, *t*-test).

Individual Neurons Discharge Differently During Two Locomotion Tasks

Upon transition from simple locomotion to walking along the horizontal ladder, individual neurons changed their activity to even a greater extent than the populations did as a whole: 79% of neurons changed at least one characteristic of the activity. First, the mean discharge rate changed in 42% (100/238) of neurons, increasing in 19% (46/238) of neurons and decreasing in 23% (54/238) (Fig. 9*A*). The increase was on average 63 ± 55%, and the decrease was 34 ± 16%. The peak discharge rates averaged over one histogram bin (1/20th of the cycle) also changed in many neurons upon transition from simple to ladder locomotion. They increased in 30% of cells (68 of 230 neurons whose activity was step related in at least one of the tasks) and decreased in 14% (33/230). The average increase was 20.5 ± 9.0 (73 ± 53%) and the decrease was 16.5 ± 6.5 (32 ± 15%) spikes/s, respectively.

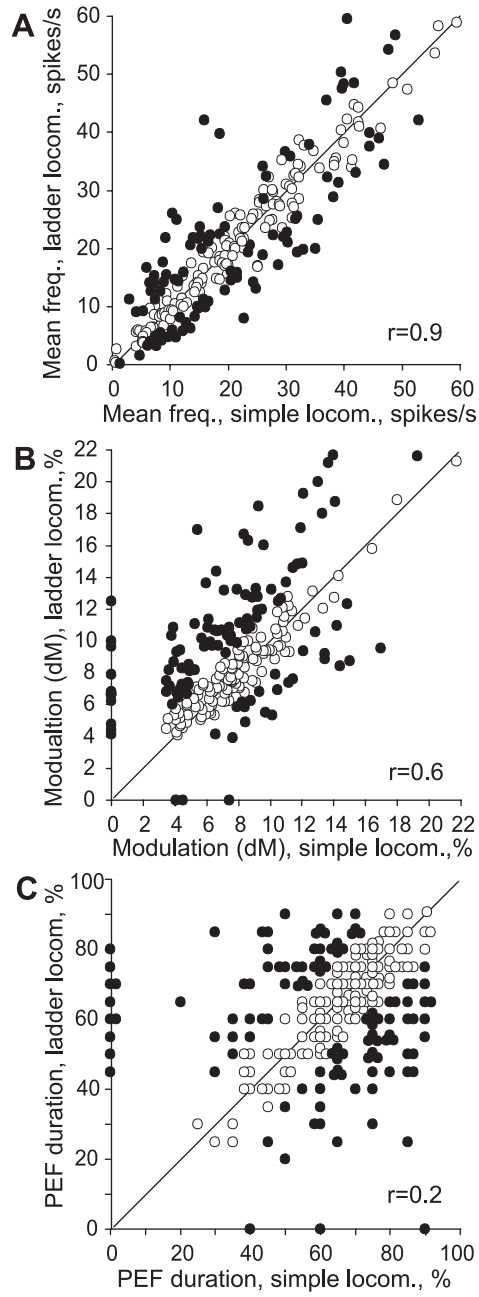

Fig. 9. Comparison of activity characteristics of individual neurons during simple and ladder locomotion. The *x*- and *y*-axes of each point show the values of a characteristic of a neuron during simple and ladder locomotion, respectively. Neurons whose characteristics were statistically significantly different during the 2 tasks are shown by filled circles; the others are shown by open circles. *A*: mean discharge frequency averaged over the stride. *B*: coefficient of frequency modulation, dM. *C*: duration of PEF. For two-PEF neurons, the combined duration of two PEFs is given. The coefficient of correlation (*r*) is indicated.

Second, the strength of frequency modulation changed in an even larger fraction of cells than the mean or peak rates: it increased in 44% of cells (96 of 217 neurons modulated in both tasks; $P < 0.01$, χ^2-test) and decreased in 11% (24/217). The dM increases ranged from 20% to 200% of the value observed during simple locomotion and were 57 ± 37% on average, while the decreases were 33 ± 10%. In contrast to the scatterplot of mean frequencies (Fig. 9*A*), data points in the plot for

dM (Fig. 9*B*) were more widely distributed along the *y*-axis. The increase in M was 15 ± 8% on average.

Third, the duration of the PEF changed in 44% of neurons (96/217), decreasing in 24% (52/217) and increasing in 20% (44/217) of them by 15–50% of the cycle. In many neurons, the duration of the PEF differed considerably between simple and ladder locomotion, and there was no correlation between these two values ($r = 0.2$; Fig. 9*C*).

Fourth, the preferred phase of activity changed in 26% of one-PEF neurons (in 38 of 145 cells modulated with 1 PEF in both tasks; see Fig. 11*A*), and the phase positions of individual PEFs changed in some two-PEF cells. In addition, the number of PEFs per cycle changed in many neurons. Close to half (43%, 30/69) of neurons with a two-PEF pattern during simple locomotion had one PEF during ladder locomotion (see Fig. 12, *A* and *B*). Also, 15% (22/148) of neurons that had one PEF during simple locomotion had two PEFs on the ladder (Fig. 12, *C* and *D*).

Finally, 10 neurons were involved in the locomotion-related activity during the ladder task only, and three neurons lost their modulation during walking on the ladder. We will consider further the changes in the discharges of individual neurons separately for the cells active in the same phase during both locomotion tasks and for the cells that were active in different phases.

Neurons active in the same phase during both tasks. The preferred phases of activity in half of one-PEF neurons (80/148, 54%) did not change upon transition from simple to ladder locomotion, whereas other parameters of the discharge could change (Fig. 10). Most striking was the change in the strength of stride-related modulation. In 24 (30%) neurons its value increased by 50 ± 30%. Along with this increase, either the average discharge rate or the duration of PEF often changed. Both tended to decrease as the depth of modulation increased. At the same time, the peak discharge rate and the average activity within the PEF typically increased (by 10–35 spikes/s) or did not change. There were also five cells in which the duration of the PEF decreased without a change in the strength of modulation. Thus, during complex locomotion, the activity of 36% (29/80) neurons with one PEF during both locomotion tasks became more task related as well as more time restricted, better tuned to a particular phase of the step cycle, and more precise (compare Fig. 6, *A* and *B* and *G* and *H*); we have termed these cells *group I* neurons. *Group I* neurons projected to both distal and proximal forelimb representations in the motor cortex and had a variety of conduction velocities and receptive fields. Two-thirds of them were located medially in the VL. The preferred phases of activity of *group I* neurons were distributed evenly across the stride. Another 10% (8/80) of neurons decreased their modulation depth during ladder locomotion by 30 ± 8% on average. Besides these, 24% (19/80) of cells changed their discharge rate without altering the depth of modulation or PEF duration, and another 24% (19/80) discharged similarly during two locomotion tasks.

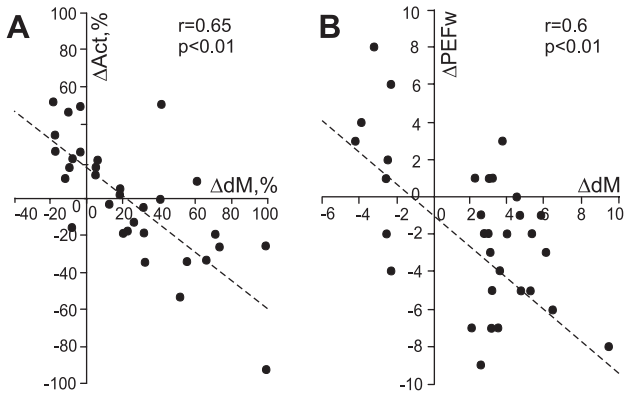

Fig. 10. Changes in activity characteristics of neurons that were active in similar phases of the stride and had one PEF during both simple and ladder locomotion. *A*: negative correlation between change in the depth of modulation (dM) and mean discharge frequency (Act). *B*: negative correlation between the change in the depth of modulation and duration of PEF (PEFw). In *A* and *B* the *x*-axis and *y*-axis of each point show the difference in a discharge characteristic of a neuron between simple and ladder locomotion tasks. The difference is positive if the value of the parameter was larger during ladder locomotion. Only neurons with statistically significant difference in the depth of modulation between two tasks are shown. The coefficient of correlation (r) is indicated.

Half of two-PEF neurons (38/69, 55%) also did not change their phases of activity upon transition from simple to complex locomotion (e.g., Fig. 8, *A* and *B* and *F* and *G*). Discharges of 36% (25/69) of these were different during the two tasks in other aspects, however. Similar to one-PEF cells, 16 (23%) of these neurons had stronger modulation, shorter PEFs, or both during ladder locomotion, while mean activity could either increase or decrease. We have named these *group II* neurons. All but one of these neurons projected to the distal forelimb representation in the motor cortex. *Group II* neurons had a variety of axonal conduction velocities, and their receptive fields could be on either distal or proximal segments of the forelimb. Swing, stance, and transition neurons were all represented in this group.

Neurons active in different phases during two tasks. A change in the phase of activity of a neuron upon transition from simple to complex locomotion could occur either because of a phase shift of the same discharge pattern within the cycle or because of re-formation of the pattern, so that the neuron had a one-PEF pattern in one locomotion task and a two-PEF pattern during another task.

Phase shifts of the discharge pattern were seen almost exclusively in one-PEF neurons. The preferred phase in 38 (26%, 38/148) one-PEF neurons changed between two tasks in this manner (Fig. 11). We have named these *group III* neurons. The average phase shift in *group III* neurons was 20 ± 9% of the cycle (Fig. 11*A*). Approximately similar numbers of neurons discharged earlier and later in the cycle during ladder versus simple locomotion (Fig. 11*A*). Figure 11, *C–F*, illustrate two most common types of phase shifts. Aside from the preferred phase shift, the most striking modification in the activity of *group III* neurons was a change in the strength of stride-related modulation. It increased in 50% (19/38) of neurons by 65 ± 30% on average. This was similar to the behavior of *group I* neurons. In *group III*, however, the average discharge rate was typically similar during both locomotion tasks, while the duration of PEF was also shorter in more than half of the cells (Fig. 11*B*). Thus, during complex locomotion, the activity of very many *group III* neurons became also more strongly stride related and often more focused on a specific phase, precise, compared with simple locomotion. *Group III* neurons had a variety of receptive fields, but elbow extension was disproportionally represented. The great

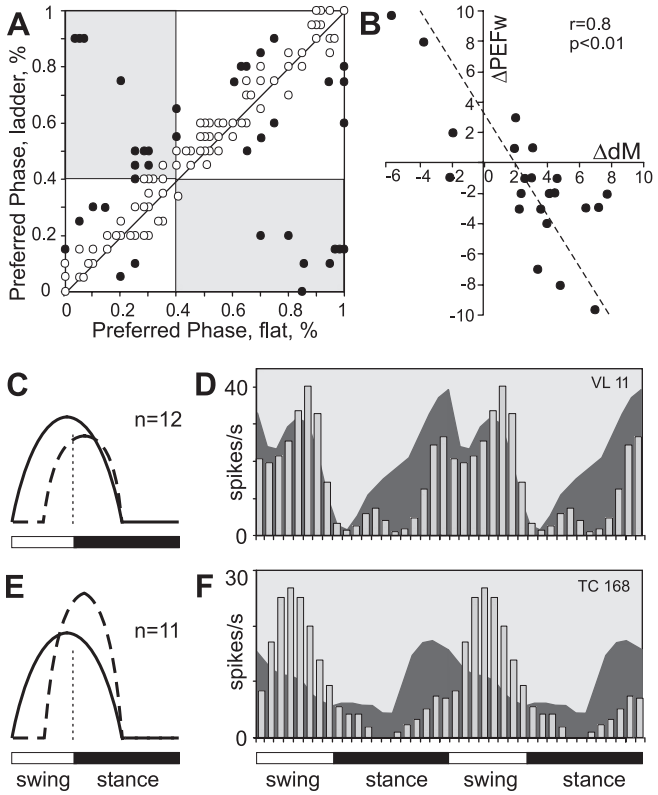

Fig. 11. Changes in activity characteristics of neurons that had one PEF during both simple and ladder locomotion but were active in different phases of the stride (*group III* neurons). *A*: comparison of preferred phases of activity in individual neurons during simple and ladder locomotion. The *x*-axis and *y*-axis of each point show the preferred phase of a neuron during simple and ladder locomotion, respectively. Neurons whose characteristics were statistically significantly different during the two tasks are shown with filled circles; the others are shown with open circles. Areas that correspond to the swing phase during one task but stance phase during the other task are shaded. *B*: negative correlation between the change in the depth of modulation and the duration of PEF. The *x*-axis and *y*-axis of each point show the difference in a discharge characteristic of a neuron between simple and ladder locomotion. The difference is positive if the value of the parameter was larger during ladder locomotion. Only neurons with statistically significant differences in the depth of modulation between two tasks are shown. The coefficient of correlation (r) is indicated. *C*: schematic presentation of the most frequently observed type of the change in the discharge pattern of *group III* neurons upon transition from simple to ladder locomotion: the shift in the preferred phase occurs because the activity in a part of the PEF observed during simple locomotion decreases during ladder locomotion. Solid line shows the activity during simple locomotion; interrupted line shows the activity during ladder task. Vertical dashed line shows the transition between swing and stance. *D*: example of activity of a typical *group III* neuron. Area histogram shows the activity of the neuron during simple locomotion. Bar histogram shows its activity during ladder task. To promote visualization of the difference between activities in two tasks, the cycle is repeated twice. *E* and *F*: same as *C* and *D* but showing the second most frequent type of the activity change in *group III* neurons when the shift in the preferred phase occurs because the activity in a part of the PEF observed during simple locomotion decreases during ladder locomotion, and this reduction is accompanied by an increase in the discharge rate during the remaining part of the PEF.

majority of *group III* neurons projected to the distal forelimb area of the motor cortex; 75% of *group III* TCs were "slow," and two-thirds of *group III* cells were located laterally within the nucleus.

Some neurons with one PEF during simple locomotion changed the preferred phase of activity on the ladder because of acquisition of a second PEF (22/148, 15%). We have named these *group IV* neurons. Figure 12, *A–D*, illustrates the two most common types of phase shifts. There was no particular phase in which the new PEF would tend to appear, and during ladder locomotion the number of *group IV* cells active in each phase of the cycle remained the same as during simple locomotion. And once again, besides the change in the pattern of modulation, the other major modification in the activity of these neurons was an increase of modulation: in 45% of group IV neurons, it increased by 74 ± 43% on average. *Group IV* neurons had a variety of receptive fields, projected to both distal and proximal forelimb representations in the motor

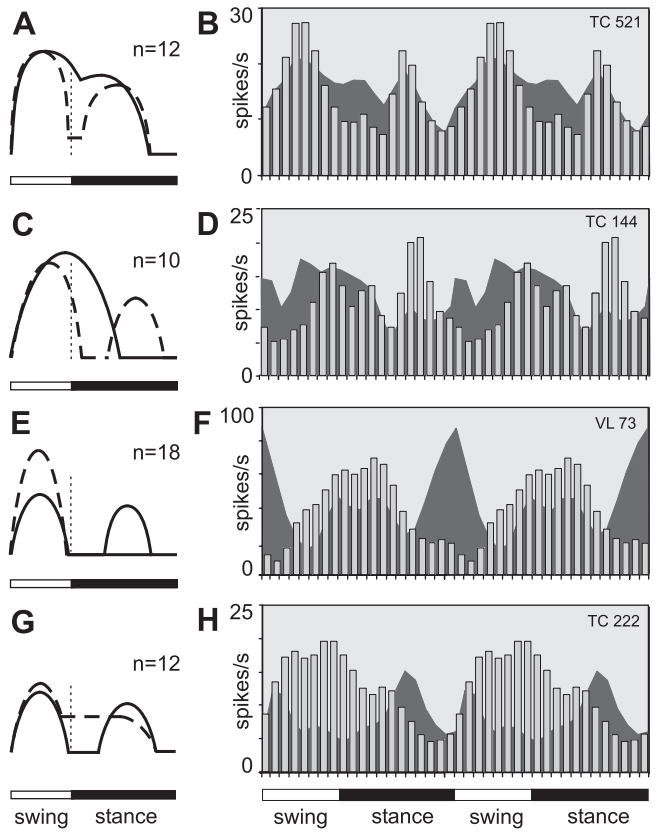

Fig. 12. Changes in the activity characteristics of neurons that had different numbers of PEFs during different locomotion tasks (*group IV* and *group V* neurons). *A*: schematic presentation of the most frequently observed type of change in the discharge pattern of *group IV* neurons upon transition from simple to ladder locomotion. The change in the number of PEFs occurs because 2 small subpeaks in the PEF during simple locomotion are shaped into 2 full PEFs. This occurs most often by deepening the trough between the subpeaks, but also through a further increase in the discharge rate within these peaks. Solid line shows activity during simple locomotion, and interrupted line shows the activity during ladder task. Vertical dashed line shows transition between swing and stance. *B*: example of the activity of a typical *group IV* neuron. Area histogram shows the activity of the neuron during simple locomotion. Bar histogram shows its activity during the ladder task. To promote visualization of the difference in activities between two tasks, the cycle is repeated twice. *C* and *D*: same as *A* and *B* but showing the second most frequent type of activity change in group IV neurons. The change in the number of PEFs occurred because the PEF observed during simple locomotion asymmetrically changed in amplitude and became shorter, and a new PEF appeared in a former trough. *E* and *F*: same as *A* and *B* but showing the most frequent type of activity change in *group V* neurons. *G* and *H*: same as *A* and *B* but showing the second most frequent type of activity change in *group V* neurons.

cortex, and nearly all *group IV* TCs were "slow." Two-thirds of *group IV* cells were located laterally in the VL.

In contrast to one-PEF neurons that only infrequently acquired a second PEF, the two-PEF cells often changed their discharge pattern ($P < 0.0001$, χ^2-test). Nearly half of neurons (30/69, 43%) with two PEFs during simple locomotion had one PEF during walking on the ladder (Fig. 12, *E–H*). We have named these *group V* neurons. In 18 of these neurons the reduction in PEF number occurred because one of the PEFs seen during simple locomotion was absent on the ladder (Fig. 12, *E* and *F*). In the overwhelming majority of the neurons ($n = 14$) this was accompanied by an increase in the discharge rate within the remaining PEF. In 12 other cells the transition from a two-PEF to a one-PEF pattern was accomplished by an increase in the activity during one of the inter-PEF intervals, joining the previously distinct PEFs (Fig. 12, *G* and *H*). There was no particular phase preference for which PEF tended to disappear in different neurons, and on the ladder the number of *group V* cells active in each phase of the cycle remained about the same as during simple locomotion, despite the fact that on the ladder they had only one PEF instead of two. The other major modification in the activity of *group V* neurons was the change in the depth of modulation. It increased in one-third of the cells by an average 72 ± 56%. *Group V* neurons projected to both distal and proximal forelimb representations in the motor cortex, had a variety of conduction velocities, and were scattered across the nucleus, but almost all had receptive fields on the shoulder.

DISCUSSION

VL Signals Conveyed During Simple Locomotion

The first goal of this study was to elucidate whether during locomotion VL neurons discharge in a manner that is suitable to contribute to the locomotion-related activity in the motor cortex. We found that they do. The activity of 92% of VL neurons was modulated in the rhythm of strides, and 67% of neurons, including 63% of TCs, discharged with a single period of elevated firing (PEF) per cycle. This discharge pattern is similar to that observed in the majority of neurons in the motor cortex (Armstrong and Drew 1984; Beloozerova and Sirota 1985, 1993a, 1993b; Drew 1993). Thus the one-PEF TCs can directly contribute to the activity in the motor cortex during locomotion. All phases of the step cycle are covered with a nearly equal neuronal representation (Fig. 6, *C*, *D*, and *F*) and similar intensity (Fig. 6*E*). A substantial number of VL neurons discharge with two PEFs per stride, including 35% of TCs. Since a limb central pattern generator (CPG) discharges only one time per cycle (reviewed in McCrea and Rybak 2008), if a neuron discharges more than once, this means that it receives input from more than one limb CPG or that there are several peripheral inputs that significantly influence its discharge. The two-PEF pattern is less frequently observed in the motor cortex (Armstrong and Drew 1984; Beloozerova and Sirota 1985, 1993a, 1993b; Drew 1993). However, in most two-PEF VL neurons one of the PEFs is typically shorter and weaker (Fig. 8*E*) and might lack a sufficient effect on the activity of the target cortical neurons.

We found two notable differences in the activity of VL neurons and efferent neurons of motor cortex layer V. The average depth of modulation (dM) is lower in the VL, 8 ± 0.2% vs. 10 ± 0.7% (Sirota et al. 2005; $P < 0.05$, *t*-test), and the discharge within the activity bursts is more variable. That is, stride-related responses of VL neurons are less phase specific compared with those of motor cortex layer V neurons. This agrees with previous findings of a weaker directional specificity of VL neuron discharges during arm and wrist movements compared with that of neurons in the motor cortex (Kurata 2005; Strick 1976) and is in line with an analogous observation in the visual system, where responses of neurons in the lateral geniculate nucleus are less specific to visual stimuli than those of cells in the visual cortex (see, e.g., Tsao and Livingstone 2008).

The locomotion-related modulation of activity in the VL during simple locomotion may arise from two main sources: the spino-thalamic projection (Craig 2008; Mackel et al. 1992; Yen et al. 1991) and the cerebello-thalamic projection (Evrard and Craig 2008; Ilinsky and Kultas-Ilinsky 1984; Nakano et al. 1980; Steriade 1995). In addition, influence from the motor cortex may partially contribute. In decerebrated cats, it was found that the cerebellum plays the pivotal role in driving locomotion-related discharges in neurons of subcortical motor centers, including neurons of the red and vestibular nuclei, and neurons of reticular formation giving rise to the reticulo-spinal tract (Orlovski 1970; Orlovsky 1972a, 1972b; reviewed in Arshavsky et al. 1986). It can be suggested that the VL, another subcortical motor nucleus receiving direct connections from the cerebellum, does not differ in this respect. Indeed, the cerebellum receives information both from the spinal locomotor CPG and from somatosensory receptors (Arshavsky et al. 1986; Lundberg and Oscarsson 1962; Oscarsson 1965) and can pass both types of information to the VL. All deep cerebellar nuclei project to the area of VL that we have explored (see, e.g., Angaut 1979; Evrard and Craig 2008; Ilinsky and Kultas-Ilinsky 1984; Nakano et al. 1980; Rinvik and Grofová 1974; Rispal-Padel and Grangetto 1977), and it was shown that all these nuclei house neurons whose activity is strongly step related during locomotion (Armstrong and Edgley 1984; Nilaweera and Beloozerova 2009; Orlovski 1972). Interposed nucleus neurons more often (57% of cells) discharge one burst of spikes per stride, while 39% discharge two bursts (Armstrong and Edgley 1984). These proportions are similar to those that we found in the VL ($P > 0.05$, χ^2-test). Also, similarly to VL neurons, periods of elevated firing in interposed nucleus neurons are widely distributed through the stride, and as a population they too have a slightly elevated activity during swing phase. Lateral nucleus neurons usually have a single PEF, and their preferred phases are also distributed across the step cycle (Beloozerova and Sirota 1998; Nilaweera and Beloozerova 2009).

VL Signals Conveyed During Complex Locomotion

The second goal of the present study was to explore whether VL neurons discharge in a manner that is suitable to contribute to the additional modulation of the activity in the motor cortex that occurs during locomotion over complex terrain. Do VL neurons transmit to the motor cortex signals that are needed to control the landing positions of feet during walking on a complex terrain? We found that the activity of VL neurons with one PEF was modulated more strongly on the ladder than

during simple locomotion. The fast-conducting TCs and neurons with preferred phases in the first half of swing during simple locomotion increased their activity during swing, while the slow-conducting TCs and shoulder-related cells became more active during stance (Fig. 7). The overwhelming majority of individual one-PEF and two-PEF neurons changed their discharges upon transition from simple to complex locomotion. The dominant change, similar to that in the motor cortex, was an increase in the depth and temporal precision of the modulation (Fig. 9, *B* and *C*). In contrast to simple walking, during complex locomotion the depth of modulation in VL neurons was as high as in the motor cortex efferent population of layer V: 9.6 ± 0.3% vs. 11 ± 0.8% (Sirota et al. 2005; $P > 0.05$, *t*-test). The further increase in the similarity between VL and motor cortex discharges during complex locomotion suggests that the VL may have a significant contribution to the modulation of the motor cortex activity during this task.

The VL appears to be more than a simple relay for signals passing to the motor cortex during complex locomotion. Many of the VL neurons discharged in different phases of the cycle during simple and complex locomotion. This shows that the information related to the complex environment changes the basic locomotion-related discharge pattern of VL neurons. Five major modes of integration can be recognized.

The first two modes were represented in the activity of neurons of *groups I* and *II*, respectively (Fig. 6, *A* and *B* and *F* and *G*; Fig. 8, *A* and *B* and *F* and *G*; Fig. 13). These were adjustments of the modulation (with 1 PEF or 2 PEFs, respectively) with regard to magnitude only. In the activity of *group I* and *II* neurons the simple locomotion-related pattern was dominant, and the role of complex locomotion-related information was to increase the activity level and the efficacy of the stride-related modulation. These modes of integration could either occur in the cerebellum, with results transmitted to the VL, or take place in the VL itself. Having large numbers of neurons whose activity patterns retain their phase position within the step cycle might be beneficial for smooth performance of complex movements such as locomotion in challenging environments.

The third mode of integration was "fine-tuning" of timing of the activity, as seen in *group III* neurons (Fig. 11 and Fig. 13). The simple locomotion-related information also dominated the activity of these neurons, but on the ladder its timing was slightly adjusted by complex locomotion-related input. We hypothesize that this assisted in proper timing of foot placements on the crosspieces of the ladder.

The fourth mode of integration was the conversion of two-PEF neurons into one-PEF neurons (Fig. 12, *E–H*, and Fig. 13). In this mode, the simple and complex locomotion-related information had approximately equal roles, with the simple locomotion-related information still having a significant contribution to determining the discharge timing of the neuron and with the complex locomotion-related information substantially altering it. Conversion of two-PEF neurons into one-PEF neurons aligned the discharge pattern of VL neurons with that of cells in the motor cortex and presumably increased the efficacy of VL influences upon the motor cortex.

The fifth mode of integration was a summation of simple and complex locomotion-related inputs coming in different phases of the stride (Fig. 11, *A–D*, and Fig. 13). Here the simple and complex locomotion-related information also had approximately equal roles, and the complex locomotion-based information simply supplemented the existing simple locomotion-based pattern. This changed phasing of neuron activity, and we hypothesize that it assisted in accurate timing of foot placements during complex locomotion.

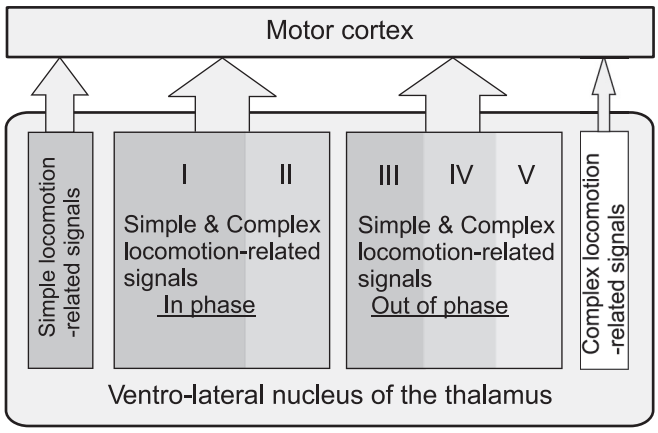

Fig. 13. Signals conveyed from the VL to the motor cortex during locomotion. See DISCUSSION for details.

Nature of Signals Conveyed by the VL During Complex Locomotion

What is the content of the complex locomotion-related information conveyed by the VL to the motor cortex during complex locomotion? We have previously demonstrated that the mechanics of simple locomotion on the flat surface and complex locomotion along the horizontal ladder used in our studies are rather similar (Beloozerova et al. 2010). The crosspieces of the ladder are positioned at comfortable distances, and their tops are flat and wide enough to easily accommodate the foot. Under these conditions, in the forelimbs, there are only slight differences in the wrist movements and in the activity of some wrist-related muscles between simple and complex locomotion. One can hypothesize, however, that largely similar movements of simple and ladder locomotion still produce different proprioceptive afferentation, which is then transmitted to the motor cortex via the VL. It was shown that the level of fusimotor activity is often higher during difficult motor tasks, especially those that are novel, strenuous, or associated with a high degree of uncertainty (Hulliger et al. 1989; Prochazka et al. 1988). Our ladder locomotion task was well practiced, however, entirely predictable, and, judging from levels of EMG activity (Beloozerova et al. 2010), not at all strenuous. Thus it does not seem very likely that a potential difference in the proprioceptive afferentation between simple and ladder locomotion can be responsible for the entire volume and spectrum of discharge differences of VL neurons during these two tasks.

In addition to moving the wrist slightly differently during simple and ladder locomotion, on the ladder cats assume a more bent-forward posture by lowering the center of mass and rotating the neck down. These differences in the activity of very proximal as well as very distal limb muscles, albeit small, can be sensed by neurons in the VL and conveyed to the motor cortex. Indeed, we found that during ladder locomotion the population of neurons responsive to passive movements in the shoulder joint and/or palpation of back, chest, or neck muscles reorganizes its activity compared with simple walking (Fig. 7,

A and *D*). It could then be expected that, similarly, the activity of the wrist-related population will also reflect the difference in kinematics in this joint during the two locomotion tasks. We did not see this, however. Although many individual wrist-related neurons changed their activity between the tasks, as a group the activity of this population was similar during simple and complex locomotion (Fig. 7, *C* and *F*). This can be explained by the too small difference in the kinematics between the tasks. Alternatively, it can be suggested that the activity of some neurons in the VL is not directly related to mechanics of the movements and somatosensation.

While differences in mechanics of locomotion between simple and ladder tasks are on the small side, and the relationship of the activity of VL neurons to those differences is inconsistent, cats move their eyes and look at the walking pathway in a very different manner during simple and ladder locomotion (Beloozerova et al. 2010; Rivers et al. 2009). Cats only infrequently look at the surface of the pathway when it is flat, but they intensively inspect the surface on every single run when walking along the ladder. Moreover, on the ladder there is a correlation between timing of gaze shifts and stride phase (Rivers et al. 2010). Similar data have been reported for humans walking on stepping-stones (Hollands et al. 1995; Hollands and Marple-Horvat 2001). Considering the rather similar limb motor patterns in the two locomotion tasks but dramatically different gaze behaviors, we want to suggest that at least a part of the differences in discharges of VL neurons during simple and ladder locomotion reflects differences in processing of visual information during these two tasks, as well as the changes in motor commands made on the basis of visual information. During locomotion in a complex environment visual information about the position of the stepping target is first processed through visual networks and then at some point is incorporated into the basic locomotion rhythm in order to guide the limb. From this point on it becomes integrated "visuo-motor" information that, in the afferent sense, is "[processed] visual information," while in the efferent sense it is a "limb control signal" reflecting preparation of the movement. It has been suggested that visual information about the environment is integrated with movement-related information in the cerebellum and then funneled to the motor cortex via the VL for control of limb movements (Glickstein 2000; Glickstein and Gibson 1976; Stein and Glickstein 1992). Martin and Ghez (1985) had found earlier that the onset of elbow movement-related activity in many motor cortical neurons, although indeed well time related to the movement, is even better time locked to the visual trigger stimulus. On the basis of anatomical evidence, the authors suggested that the most likely pathway to convey such processed visual information to the motor cortex is the VL.

Relative Contribution of Signals from VL and Associative Cortex to Motor Cortex Activity During Visually Guided Locomotion

Two sources of signals that modify the stride-related modulation of neuronal activity in the motor cortex during locomotion over a complex terrain can be suggested: cortical and subcortical. While the VL appears to be well suited to supply the motor cortex throughout the entire step cycle with synthesized vision-related information thus determining the motor cortex's overall activity outline, direct projections from associative cortical areas are likely to provide a more specific shaping.

Research in nonhuman primates has shown that neurons in the cortical area 6, the premotor cortex, discharge in close relationship with reaching movements to visual targets (see, e.g., Crammond and Kalaska 1994, Wise et al. 1992). Area 6 has substantial inputs from parietal visual areas as well as direct cortico-cortical projections to the motor cortex (Ghosh 1997; Jones et al. 1978; Marconi et al. 2001). So far only one study has examined the activity of area 6 during treadmill locomotion (Criado et al. 1997). It was found that 59% of neurons in area 6 change their discharge rate with the start of locomotion, typically by increasing it. The discharge of only ~30% of these cells, however, is stride related during locomotion. In addition, nearly all step-related area 6 cells discharge predominantly during the stance phase of the stride. Thus, although area 6 neurons may influence the motor cortex and VL during stance, when it is believed that planning of the next limb transfer takes place (Laurent and Thomson 1988; Hollands and Marple-Horvat 1996), they cannot be responsible for the majority of swing and transition phase-related activity in either the motor cortex or VL.

Regarding direct cortico-cortical projections from parietal area 5 to the motor cortex, although they are numerous (see, e.g., Andujar and Drew 2007; Babb et al. 1984; Caria et al. 1997; Mori et al. 1989), at least those that come from layer III of area 5b carry rather low activity during both simple and complex locomotion, both in terms of proportion of neurons involved (~50%) as well as their average discharge rates (~1 spikes/s; Beloozerova et al. 2011). The potential for the parietal area 5 to supply the motor cortex with vision-based information during complex locomotion has been considered in detail in our previous publication (Beloozerova and Sirota 2003). We have concluded that the activity of this area is not well suited to directly determine the great majority of the locomotion-related responses in the motor cortex. On the basis of data obtained in experiments with cats overstepping a moving obstacle on the treadmill, a suggestion that area 5 is most likely to exert its influence on locomotion mechanism via subcortical motor centers such as basal ganglia or lateral cerebellum has been also made by Andujar and colleagues (2010). The role of the sparse direct projection from area 5 to the motor cortex during complex locomotion is yet to be determined.

Overall, available data suggest that subcortical routes that link visual and motor cortex areas participate very importantly in transmission of vision-based signals that modify stride-related modulation of neuronal activity in the motor cortex during complex locomotion. The pathway that runs via the pons, cerebellum, and VL is the largest of all subcortical links between visual and motor cortices. In this study we investigated signals that are conveyed from the VL to the motor cortex during visually guided locomotion. We suggest that they have significant contribution.

ACKNOWLEDGMENTS

The authors are grateful to Dr. Galina A. Pavlova for acquisition of a part of the data and to Peter Wettenstein for exceptional engineering assistance. We are also indebted to Drs. Alan R. Gibson, Kris M. Horn, and Vladimir K. Berezovskii for help in processing and analysis of our morphological data. Fluorescent imaging was supported by National Eye Institute Grant P30 EY-12196 and performed at Harvard University Medical School.

GRANTS

This research was supported by National Institute of Neurological Disorders and Stroke Grants R01 NS-39340 and R01 NS-058659 to I. N. Beloozerova.

DISCLOSURES

No conflicts of interest, financial or otherwise, are declared by the author(s).

AUTHOR CONTRIBUTIONS

Author contributions: V.M., M.G.S., and I.N.B. conception and design of research; V.M., W.U.N., and I.N.B. performed experiments; V.M., W.U.N., P.V.Z., M.G.S., and I.N.B. analyzed data; V.M., M.G.S., and I.N.B. interpreted results of experiments; V.M. and I.N.B. prepared figures; V.M. and I.N.B. drafted manuscript; V.M., M.G.S., and I.N.B. edited and revised manuscript; V.M., W.U.N., P.V.Z., M.G.S., and I.N.B. approved final version of manuscript.

REFERENCES

Andujar JE, Lajoie K, Drew T. A combination of area 5 of the posterior parietal cortex to the planning of visually guided locomotion: limb-specific and limb-independent effects. *J Neurophysiol* 103: 986–1006, 2010.

Andujar JE, Drew T. Organization of the projections from the posterior parietal cortex to the rostral and caudal regions of the motor cortex of the cat. *J Comp Neurol* 504: 17–41, 2007.

Angaut P. The cerebello-thalamic projection in the cat. In: *Cerebro-Cerebellar Interactions*, edited by Massion J, Sasaki K. Amsterdam: Elsevier North-Holland, 1979, p. 1943.

Armstrong DM, Drew T. Discharges of pyramidal tract and other motor cortical neurons during locomotion in the cat. *J Physiol* 346: 471–495, 1984.

Armstrong DM, Edgley SA. Discharges of nucleus interpositus neurones during locomotion in the cat. *J Physiol* 351: 411–432, 1984.

Armstrong DM, Drew T. Electromyographic responses evoked in muscles of the forelimb by intracortical stimulation in the cat. *J Physiol* 367: 309–326, 1985.

Armstrong DM, Marple-Horvat DE. Role of the cerebellum and motor cortex in the regulation of visually controlled locomotion. *Can J Physiol Pharmacol* 74: 443–455, 1996.

Arshavsky YI, Gelfand IM, Orlovsky GN. *Cerebellum and Rhythmical Movements*. Berlin: Springer, 1986.

Asanuma H, Hunsperger RW. Functional significance of projection from the cerebellar nuclei to the motor cortex in the cat. *Brain Res* 98: 73–92, 1975.

Asanuma C, Thach WT, Jones EG. Cytoarchitectonic delineation of the ventral lateral thalamic region in the monkey. *Brain Res* 286: 219–235, 1983.

Babb RS., Waters RS, Asanuma H. Corticocortical connections to the motor cortex from the posterior parietal lobe (areas 5a, 5b, 7) in the cat demonstrated by the retrograde axonal transport of horseradish peroxidase. *Exp Brain Res* 54 476–484, 1984.

Batshelet E. *Circular Statistics in Biology*. London: Academic, 1981.

Beloozerova IN, Sirota MG. [Activity of neurons of the motosensory cortex during natural locomotion in the cat]. *Neirofiziologia* 17: 406–408, 1985.

Beloozerova IN, Sirota MG. Role of motor cortex in control of locomotion. In: *Stance and Motion. Facts and Concepts*, edited by Gurfinkel VS, Ioffe ME, Massion J, Roll JP. New York: Plenum, 1988, p. 163–176.

Beloozerova IN, Sirota MG. The role of the motor cortex in the control of accuracy of locomotor movements in the cat. *J Physiol* 461: 1–25, 1993a.

Beloozerova IN, Sirota MG. The role of the motor cortex in the control of vigour of locomotor movements in the cat. *J Physiol* 461: 27–46, 1993b.

Beloozerova IN, Sirota MG. Cortically controlled gait adjustments in the cat. *Ann NY Acad Sci* 860:550–553, 1998.

Beloozerova IN, Sirota MG. Activity of ventrolateral thalamus (VL) during locomotion (Abstract). *Soc Neurosci Abstr* 28: 62.–13, 2002.

Beloozerova IN, Sirota MG. Integration of motor and visual information in the parietal area 5 during locomotion. *J Neurophysiol* 90: 961–971, 2003.

Beloozerova IN, Sirota MG, Swadlow HA. Activity of different classes of neurons of the motor cortex during locomotion. *J Neurosci* 23: 1087–1097, 2003.

Beloozerova IN, Sirota MG, Orlovsky GN, Deliagina TG. Activity of pyramidal tract neurons in the cat during postural corrections. *J Neurophysiol* 93: 1831–1844, 2005.

Beloozerova IN, Farrell BJ, Sirota MG, Prilutsky BI. Differences in movement mechanics, electromyographic, and motor cortex activity between accurate and non-accurate stepping. *J Neurophysiol* 103: 2285–2300, 2010.

Beloozerova IN, Nilaweera WU, Viana di Prisco G, Sirota MG, Marlinski V. Sparse locomotion-related activity of cortico-cortical projection from parietal area 5 to motor cortex. *Soc Neurosci Abstr*, 2011.

Bishop PO, Burke W, Davis R. The identification of single units in central visual pathways. *J Physiol* 162: 409–431, 1962.

Buneo CA, Andersen RA. The posterior parietal cortex: sensorimotor interface for the planning and online control of visually guided movements. *Neuropsychologia* 44: 2594–2606, 2006.

Caria MA, Kaneko T, Kimura A, Asanuma H. Functional organization of the projection from area 2 to area 4gamma in the cat. *J Neurophysiol* 77: 3107–3114, 1997.

Craig AD. Retrograde analyses of spinothalamic projections in the macaque monkey: input to the ventral lateral nucleus. *J Comp Neurol* 508: 315–328, 2008.

Crammond DJ, Kalaska JF. Modulation of preparatory neuronal activity in dorsal premotor cortex due to stimulus-response compatibility. *J Neurophysiol* 71: 1281–1284, 1994.

Criado JM, de la Fuente A, Heredia M, Riolobos AS, Yajeya J. Electrophysiological study of prefrontal neurones of cats during a motor task. *Pflügers Arch* 434: 91–96, 1997.

Drew T. Motor cortical cell discharge during voluntary gait modification. *Brain Res* 457: 181–187, 1988.

Drew T. Motor cortical activity during voluntary gait modifications in the cat. I. Cells related to the forelimbs. *J Neurophysiol* 70: 179–199, 1993.

Drew T, Doucet S. Application of circular statistics to the study of neuronal discharge during locomotion. *J Neurosci Methods* 38: 171–181, 1991.

Evarts EV. Activity of thalamic and cortical neurons in relation to learned movement in the monkey. *Int J Neurol* 8: 321–326, 1971.

Evrard HC, Craig AD. Retrograde analysis of the cerebellar projections to the posteroventral part of the ventral lateral thalamic nucleus in the macaque monkey. *J Comp Neurol* 508: 286–314, 2008.

Fisher NI. *Statistical Analysis of Circular Data*. Cambridge, UK: Cambridge Univ. Press, 1993.

Fuller JH, Schlag JD. Determination of antidromic excitation by the collision test: problems of interpretation. *Brain Res* 112: 283–298, 1976.

Ghosh S. Comparison of the cortical connections of areas 4 gamma and 4 delta in the cat cerebral cortex. *J Comp Neurol* 388: 371–396, 1997.

Gibson AR, Hansma DI, Houk JC, Robinson FR. A sensitive low artifact TMB procedure for the demonstration of WGA-HRP in the CNS. *Brain Res* 298: 235–241, 1984.

Glickstein M, Gibson AR. Visual cells in the pons of the brain. *Sci Am* 235: 90–98, 1976.

Glickstein M. How are visual areas of the brain connected to motor areas for the sensory guidance of movement? *Trends Neurosci* 23: 613–617, 2000.

Grofová I, Rinvik E. Cortical and pallidal projections to the nucleus ventralis lateralis thalami. Electron microscopical studies in the cat. *Anat Embryol (Berl)* 146: 113–132, 1974.

Hendry SH, Jones EG, Graham J. Thalamic relay nuclei for cerebellar and certain related fiber systems in the cat. *J Comp Neurol* 185: 679–713, 1979.

Hildebrand M. Symmetrical gaits of horses. *Science* 150: 701–708, 1965.

Hollands MA, Marple-Horvat DE. Visually guided stepping under conditions of step cycle-related denial of visual information. *Exp Brain Res* 109: 343–356, 1996.

Hollands MA, Marple-Horvat DE. Coordination of eye and leg movements during visually guided stepping. *J Mot Behav* 33: 205–216, 2001.

Hollands MA, Marple-Horvat DE, Henkes S, Rowan AK. Human eye movements during visually guided stepping. *J Mot Behav* 27: 155–163, 1995.

Hulliger M, Dürmüller N, Prochazka A, Trend P. Flexible fusimotor control of muscle spindle feedback during a variety of natural movements. *Prog Brain Res* 80: 87–101, 1989.

Ilinsky IA, Kultas-Ilinsky K. An autoradiographic study of topographical relationships between pallidal and cerebellar projections to the cat thalamus. *Exp Brain Res* 54: 95–106, 1984.

Jones EG, Coulter JD, Hendry SH. Intracortical connectivity of architectonic fields in the somatic sensory, motor and parietal cortex of monkeys. *J Comp Neurol* 181: 291–347, 1978.

Kalaska JF. Parietal cortex area 5 and visuomotor behavior. *Can J Physiol Pharmacol* 74: 483–498, 1996.

Kurata K. Activity properties and location of neurons in the motor thalamus that project to the cortical motor areas in monkeys. *J Neurophysiol* 94: 550–566, 2005.

Lajoie K, Drew T. Lesions of area 5 of the posterior parietal cortex in the cat produce errors in the accuracy of paw placement during visually guided locomotion. *J Neurophysiol* 97: 2339–2354, 2007.

Lajoie K, Andujar JE, Pearson K, Drew T. Neurons in area 5 of the posterior parietal cortex in the cat contribute to interlimb coordination during visually guided locomotion: a role in working memory. *J Neurophysiol* 103: 2234–2254, 2010.

Larsen KD, McBride RL. The organization of feline entopenduncular nucleus projections: anatomical studies. *J Comp Neurol* 184: 293–308, 1979.

Laurent M, Thomson JA. The role of visual information in control of a constrained locomotor task. *J Mot Behav* 20: 17–37, 1988.

Liddell EGT, Phillips CG. Pyramidal section in the cat. *Brain* 67: 1–9, 1944.

Lundberg A, Oscarsson O. Functional organization of the ventral spinocerebellar tract in the cat. IV. Identification of units by antidromic activation from the cerebellar cortex. *Acta Physiol Scand* 54: 252–269, 1962.

Mackel R, Iriki A, Brink EE. Spinal input to thalamic VL neurons: evidence for direct spinothalamic effects. *J Neurophysiol* 67: 132–144, 1992.

Marconi B, Genovesio A, Battaglia-Mayer A, Ferraina S, Squatrito S, Molinari M, Lacquaniti F, Caminiti R. Eye-hand coordination during reaching. I. Anatomical relationships between parietal and frontal cortex. *Cereb Cortex* 11: 513–527, 2001.

Marigold DS, Patla AE. Visual information from the lower visual field is important for walking across multi-surface terrain. *Exp Brain Res* 188: 23–31, 2008.

Marple-Horvat DE, Criado JM. Rhythmic neuronal activity in the lateral cerebellum of the cat during visually guided stepping. *J Physiol* 518: 595–603, 1999.

Martin JH, Ghez C. Differential impairments in reaching and grasping produced by local inactivation within the forelimb representation of the motor cortex in the cat. *Exp Brain Res* 94: 429–443, 1993.

McCrea DA, Rybak IA. Organization of mammalian locomotor rhythm and pattern generation. *Brain Res Rev* 57: 134–146, 2008.

Mesulam MM. Principles of horseradish peroxidase neurochemistry and their applications for tracing neural pathways-axonal transport, enzyme histochemistry and light microscopic analysis. In: *Tracing Neuronal Connections with Horseradish Peroxidase*, edited by Mesulam MM. New York: Wiley, 1982, p. 1–151.

Miles OB, Cerminara NL, Marple-Horvat DE. Purkinje cells in the lateral cerebellum of the cat encode visual events and target motion during visually guided reaching. *J Physiol* 571: 619–637, 2006.

Mori A, Waters RS, Asanuma H. Physiological properties and patterns of projection in the cortico-cortical connections from the second somatosensory cortex to the motor cortex, area 4 gamma, in the cat. *Brain Res* 504: 206–210, 1989.

Mountcastle VB. The parietal system and some higher brain functions. *Cereb Cortex* 5: 377–390, 1995.

Nakano K, Takimoto T, Kayahara T, Takeuchi Y, Kobayashi Y. Distribution of cerebellothalamic neurons projecting to the ventral nuclei of the thalamus: an HRP study in the cat. *J Comp Neurol* 194: 427–439, 1980.

Nakano K, Kohno M, Hasegawa Y, Tokushige A. Cortical and brain stem afferents to the ventral thalamic nuclei of the cat demonstrated by retrograde axonal transport of horseradish peroxidase. *J Comp Neurol* 231: 102–120, 1985.

Neafsea EJ, Hull CD, Buchwald NA. Preparation for movement in the cat. II. Unit activity in the basal ganglia and thalamus. *Electroencephalogr Clin Neurophysiol* 44: 714–723, 1978.

Nilaweera WU, Beloozerova IN. Neurons of lateral nucleus of cerebellum change their step-related frequency modulation when visual control of stepping is required (Abstract). *Soc Neurosci Abstr* 35: 367.–25, 2009.

Orlovski GN. [Cerebellar influence on the reticulo-spinal neurons during locomotion] . *Biofizika* 15: 894–901, 1970.

Orlovski GN. [Activity of cerebellar nuclei neurons during locomotion]. *Biofizika* 17: 1119–1126, 1972.

Orlovsky GN. Activity of vestibulospinal neurons during locomotion. *Brain Res* 46: 85–98, 1972a.

Orlovsky GN. Activity of rubrospinal neurons during locomotion. *Brain Res* 46: 99–112, 1972b.

Orlovsky GN, Deliagina TG, Grillner S. *Neuronal Control of Locomotion. From Mollusc to Man*. New York: Oxford Univ. Press, 1999.

Oscarsson O. Functional organization of the spino- and cuneocerebellar tracts. *Physiol Rev* 45: 495–522, 1965.

Prilutsky BI, Sirota MG, Gregor RJ, Beloozerova IN. Quantification of motor cortex activity and full-body biomechanics during unconstrained locomotion. *J Neurophysiol* 94: 2959–2969, 2005.

Prochazka A, Hulliger M, Trend P, Durmuller N. Dynamic and static fusimotor set in various behavioural contexts. In: *Mechanoreceptors: Development, Structure and Function*, edited by Hnik P, Soukup T, Vejsada R, Zelena J. New York: Plenum, 1988, p. 417–430.

Pryor K. *Lads Before the Wind*. New York: Harper and Row, 1975.

Reinoso-Suarez F. *Topographischer Hirnatlas der Katze für experimental-physiologische Untersuchungen*. Darmstadt, Germany: E. Merck, 1961.

Reitboeck HJ. Fiber microelectrodes for electrophysiological recordings. *J Neurosci Methods* 8: 249–262, 1983.

Rinvik E. The corticothalamic projection from the pericruciate and coronal gyri in the cat. An experimental study with silver-impregnation methods. *Brain Res* 10: 79–119, 1968.

Rinvik E, Grofová I. Cerebellar projections to the nuclei ventralis lateralis and ventralis anterior thalami. Experimental electron microscopical and light microscopical studies in the cat. *Anat Embryol (Berl)* 146: 95–111, 1974.

Rispal-Padel L, Grangetto A. The cerebello-thalamo-cortical pathway. Topographical investigation at the unitary level in the cat. *Exp Brain Res* 28: 101–123, 1977.

Rivers TJ, Sirota MG, Guttentag AI, Ogorodnikov DA, Beloozerova IN. Gaze behaviors of freely walking cats (Abstract). *Soc Neurosci Abstr* 35: 454.–14, 2009.

Rivers TJ, Shah NA, Sirota MG, Beloozerova IN. The relationship between vertical gaze shifts and stride cycle in freely walking cats (Abstract). *Soc Neurosci Abstr* 36: 278.–3, 2010.

Robertson RT, Cunningham TJ. Organization of corticothalamic projections from parietal cortex in cat. *J Comp Neurol* 199: 569–585, 1981.

Sakai ST, Inase M, Tanji J. Comparison of cerebellothalamic and pallidothalamic projections in the monkey (*Macaca fuscata*): a double anterograde labeling study. *J Comp Neurol* 368: 215–228, 1996.

Schmied A, Bénita M, Condé H, Dormont JF. Activity of ventrolateral thalamic neurons in relation to a simple reaction time task in the cat. *Exp Brain Res* 36: 285–300, 1979.

Sherman S, Guillery RW. *Exploring the Thalamus*. New York: Academic, 2001.

Sherk H, Fowler GA. Neural analysis of visual information during locomotion. *Prog Brain Res* 134: 247–264, 2001.

Sirota MG, Swadlow HA, Beloozerova IN. Three channels of corticothalamic communication during locomotion. *J Neurosci* 25: 5915–5925, 2005.

Skinner BF. *The Behavior of Organisms: An Experimental Analysis*. New York: Appleton-Century-Crofts, 1938.

Stein JF, Glickstein M. Role of the cerebellum in visual guidance of movement. *Physiol Rev* 72: 967–1017, 1992.

Steriade M. Two channels in the cerebellothalamocortical system. *J Comp Neurol* 354: 57–70, 1995.

Strick PL. Activity of ventrolateral thalamic neurons during arm movement. *J Neurophysiol* 39: 1032–1044, 1976.

Trendelenburg W. Untersuchungen über reizlose vorübergehende Aussaltung am Zentralnervensystem. III. Die extermitaten Region der Grosshirninde. *Pflügers Arch* 137: 515–544, 1911.

Tsao DY, Livingstone MS. Mechanisms of face perception. *Annu Rev Neurosci* 31: 411–437, 2008.

Udo M, Kamei H, Matsukawa K, Tanaka K. Interlimb coordination in cat locomotion investigated with perturbation. II. Correlates in neuronal activity of Deiter's cells of decerebrate walking cats. *Exp Brain Res* 46: 438–447, 1982.

van Donkelaar P, Stein JF, Passingham RE, Miall RC. Neuronal activity in the primate motor thalamus during visually triggered and internally generated limb movements. *J Neurophysiol* 82: 934–945, 1999.

Widajewicz W, Kably B, and Drew T. Motor cortical activity during voluntary gait modifications in the cat. II. Cells related to the hindlimbs. *J Neurophysiol* 72: 2070–2089, 1994.

Wise SP, Di Pellegrino G, Boussaoud D. Primate premotor cortex: dissociation of visuomotor from sensory signals. *J Neurophysiol* 68: 969–972, 1992.

Yen CT, Honda CN, Jones EG. Electrophysiological study of spinothalamic inputs to ventrolateral and adjacent thalamic nuclei of the cat. *J Neurophysiol* 66: 1033–1047, 1991.

Yumiya H, Ghez C. Specialized subregions in the cat motor cortex: anatomical demonstration of differential projections to rostral and caudal sectors. *Exp Brain Res* 53: 259–276, 1984.

Zelenin PV, Beloozerova IN, Sirota MG, Orlovsky GN, Deliagina TG. Activity of red nucleus neurons in the cat during postural corrections. *J Neurosci* 30: 14533–14542, 2010.